Composite Structures 92 (2010) 1763–1774

Contents lists available at ScienceDirect

Composite Structures

journal homepage: www.elsevier.com/locate/compstruct

HSDT-layerwise analytical solution for rectangular piezoelectric laminated plates

Diego Amadeu F. Torres *, Paulo de Tarso R. Mendonça *

Group of Mechanical Analysis and Design – GRANTE, Department of Mechanical Engineering, Federal University of Santa Catarina, 88040-900 Florianópolis, SC, Brazil

ARTICLE INFO

Article history:
Available online 13 February 2010

Keywords:
Analytic solution
Piezoelectricity
Laminated plates
Higher-order shear deformation theory
Layerwise theory

ABSTRACT

The present paper develops a formulation for laminated plates with extensional distributed piezoelectric sensors/actuators. This formulation is based on linear electroelasticity, and an equivalent single layer is used for the mechanical displacement field, applying a Higher-Order Shear Deformation Theory (HSDT), whereas a layerwise discretization is used in the thickness direction for the electric potential. The electric and mechanical local equilibrium equations and local constitutive equations for the problem are identified. The Principle of Virtual Work is used to derive the dynamic equilibrium equations in terms of generalized forces and the consistent boundary conditions. The piezoelectric laminate constitutive equations are built and used to write the equations of motion in terms of generalized displacements. Finally, analytical solutions for simply supported square laminates with piezoelectric layers are developed. The entire laminate, composed of the base structure and piezoelectric layers, can be arbitrary orthotropic. The solution is adequate for an arbitrary number of piezoelectric layers and stacking positions. Moreover, the solution takes into account all material coefficients, whether mechanical, piezoelectric or dielectric. Analytical results are obtained for static bending, both in sensor and actuation modes, and for free vibration of symmetric cross-ply laminates with piezoelectric layers externally bonded to the plate.

1. Introduction

In general, adaptive materials have mechanical properties that are controlled by temperature, and magnetic or electrical fields, and may be applied in the conception of smart/intelligent structures endowed with self-monitoring and self-adaptation capabilities. The focus of studies devoted to the development of these smart/intelligent structures has ranged from shape control or vibration control/suppression to the self-diagnostic applications for fracture and damage detection within a structure.

Piezoelectric materials can provide to a structural system the capability of altering its response through sensing, actuation and control. By integrating surface-bonded and/or embedded actuators into structural components, desired localized strains may be induced by applying the appropriate voltage to the actuators. In this regard, the mechanical interaction between the actuators and the host structure must be fully understood.

The piezoelectric actuators used in beams and plates are generally thin rectangular elements, such that application of an electric field in the thickness direction causes changes in the lateral dimension. This effect characterizes the extensional piezoelectric actuators. These are usually bonded to the outermost surfaces of the structures to achieve effective actuation capability. On the other hand, if it is important to avoid damage by contact with the surrounding environment, embedded shear piezoelectric actuators may be used, in which case the application of an electric field in the thickness direction induces transverse shear deformation of the laminated beam, plate or sandwich structure.

In the process of testing and validating of a finite element code it is useful to have analytic solutions available for some standard cases, developed for the same kinematic model implemented in the code. A second major reason for seeking analytical solutions is that, even if they are always restricted in scope, they provide an insight into several aspects related to the physical behavior of the model. In recent years some analytical solutions have been obtained for some of the most used kinematic models of piezoelectric laminated plates, which are referred to in this section.

Several mechanical models for laminated plates with piezoelectric layers have been developed and the work described in [1,2] can be referenced as pioneer studies in this subject. Lee [3] developed a theory for laminated plates with distributed piezoelectric layers based on the Classical Laminate Plate Theory (CLPT). Wang and Rogers [4] also applied the classical lamination theory, in this case to plates with surface-bonded or embedded piezoelectric patches.

A coupled First-Order Shear Deformation Theory (FSDT) for multilayered piezoelectric plates was presented by Hwang and Wu [5]. Ray et al. [6] shows exact solutions for simply supported linear elastic laminated plates with embedded and surface-bonded distributed piezoelectric actuators. Vel and Batra [7] used the Eshelby–Stroh formalism to analyze the cylindrical bending of

* Corresponding authors. Tel.: +55 48 3721 9899.
E-mail addresses: diego.amadeu@gmail.com (D.A.F. Torres), mendonca@grante.ufsc.br (P.T.R. Mendonça).

0263-8223/$ - see front matter © 2010 Elsevier Ltd. All rights reserved.
doi:10.1016/j.compstruct.2010.02.007

laminated plates with distributed and segmented piezoelectric actuators. Vel and Batra [8] presented an exact three-dimensional solution for the static cylindrical bending of simply supported laminated plates with embedded shear piezoelectric actuators and subjected to mechanical and electric loading on the upper and lower surfaces. Vel et al. [9] presented an analytical solution for cylindrical bending vibrations of linear piezoelectric laminated plates obtained by extending the Stroh formalism to generalized plane strain vibrations.

An exact solution for the analysis of adaptive plates with distributed actuators considering a class of Piezoelectric Fiber Reinforce Composites (PFRC) was derived by Mallik and Ray [10]. According to the authors, such a class of materials would have more effective control capability due its better effective piezoelectric coefficients as compared to its monolithic constituent counterpart.

Mitchell and Reddy [11] presented a hybrid theory, and corresponding analytical solutions, based on an equivalent single layer theory, Reddy's Higher-Order Shear Deformation Theory (HSDT) [12], for the mechanical displacements and layerwise discretization of the electric potential. It should be noted that Reddy's HSDT is a C^1-continuous formulation, but most of the finite element formulations for higher order models are based on Levinson's model, which requires only C^0-continuous generalized displacements, which is the model used in the present paper to describe the mechanical displacements.

A variational asymptotic method in which the original three-dimensional piezoelectricity problem is split into an one-dimensional through-the-thickness analysis and a two-dimensional plate analysis, electromechanically coupled, have been used by Liao and Yu [13]. They transformed an asymptotically correct energy functional into a generalized Reissner–Mindlin model, in which the transverse shear strains are introduced as two additional degrees of freedom. The formulation was applied for analysis of a piezoelectric composite single layer plate, subject to cylindrical bending, considering in-plane and thickness polarization, considering prescribed electric potential on the lateral boundary, from the Ritz approximation method.

The buckling and free vibration response of symmetrically laminated hybrid angle-ply panels have been addressed by Dumir et al. [14], considering the non-linearity, in the von Kármán sense, and using the Improved Third Order Single Layer Theory of Kumari et al. [15]. The authors performed comparisons with the results obtained from the Third Order ZigZag Theory with additional layerwise terms for in-plane displacements. They also studied the steady state forced damped response of simply supported composite and sandwich panels in cylindrical bending. Nevertheless, it should be noted that this improved single layer theory demands C^1-continuity when it is applied to finite element formulations, due the derivative of the transverse displacement in the in-plane assumed displacement.

On the other hand, Moita et al. [16] have used the Higher-Order Shear Deformation Theory of Reddy [12] in their implementation of a triangular finite element plate based on the magneto-electro-elasticity, considering one degree of freedom for the electrical potential and another one corresponding to the magnetic potential, both for each element layer, and considering linear strain–displacement relations. They analyzed a simply-supported square plate under static bending and free vibration and compared some results with those obtained by Lage et al. [17]. However, an analytical development was addressed by Reddy [18] which derived a formulation considering only the piezoelectric effect but with similar kinematical hypothesis.

The present paper develops a formulation for piezoelectric laminated plates with extensional distributed sensors/actuators using a hybrid HSDT-layerwise model. This formulation is based on linear electroelasticity, and it is hybrid in the sense that an equivalent single layer is used for the mechanical displacement field, whereas a layerwise discretization is used in the thickness direction for the electric potential. Such kinematical hypothesis keep the C^0-continuity requirement for finite element implementations and have been used in Torres and Mendonça [19] for a numerical approach based on the Generalized Finite Element Method (GFEM).

The remainder of this paper is organized as follows. Section 2 presents the electric and mechanical local equilibrium equations considered for this problem. The constitutive equations are derived in Section 3. Section 4 deals with the kinematical hypotheses and Section 5 uses the Principle of Virtual Work to derive the equilibrium equations associated with the model, in terms of generalized forces, and the consistent boundary conditions. Section 6 presents the piezoelectric laminate constitutive equations which are used in Section 7 to write the equations of motion in terms of generalized unknowns. In Section 8, analytical solutions are developed for simply supported square laminates with externally bonded piezoelectric layers, for static bending, in sensor and actuation modes, and for free vibration. Each piezoelectric layer admits non-zero electric potential only at its lower surface. The applicability of the formulation is verified through numerical assessments in Section 10. Some conclusions are outlined in Section 11.

2. Equilibrium equations

Let the body forces per unit volume in Cartesian components be designated as $\mathbf{F} = \{F_x,\ F_y,\ F_z\}^T$ and the surface forces per unit area be $\mathbf{T} = \{T_x,\ T_y,\ T_z\}^T$. The superscript T indicates a transposed matrix. The internal stress state must satisfy the *Cauchy* equilibrium equations, $\mathrm{div}\,\boldsymbol{\sigma} + \overline{\mathbf{F}} = \mathbf{0}$, where the Principle of D'Alembert was applied to define the equivalent body forces per unit volume $\overline{\mathbf{F}}$, given by $\overline{\mathbf{F}} = \mathbf{F} - \rho\ddot{\mathbf{u}}$, with double dot standing for second time derivative, where $\mathbf{u}$ is the vector of displacement Cartesian components.

On the portion S_σ of the body surface, where the boundary traction $\overline{\mathbf{T}}$ is prescribed, it is necessary to verify the equilibrium conditions $\sigma_{ij}n_j = \overline{T}_i$, where $\mathbf{n} = \{n_x,\ n_y,\ n_z\}^T$ are the Cartesian components of the outward unit normal vector of the boundary.

For the development of an electro-mechanical coupled problem it is still necessary to establish that, if the material has a free electric charge $\overline{Q}_e$ per unit volume, the electric displacement is a vector field with components $\mathbf{D} = \{D_x,\ D_y,\ D_z\}^T$, which must satisfy the equilibrium condition, $\mathrm{div}\,\mathbf{D} = \overline{Q}_e$ in the domain, and $D_i n_i = \overline{q}_e$ on the portion S_q of the boundary where there exists a free electric charge $\overline{q}_e$ per unit area.

3. Constitutive equations

The coupling between the mechanical, thermal and electric fields can be established utilizing thermodynamic principles and the Maxwell relations [20]. Analogously to the deformation energy functional U_0 in the linear elasticity theory and to the free energy functional of Helmholtz Ψ_0 in thermoelasticity, the existence of a functional Φ_0 is assumed such that

$$\begin{aligned}\Phi_0(\varepsilon_{ij}, E_i, \phi) &= U_0 - \mathbf{E}\cdot\mathbf{D} - \eta\phi \\ &= \frac{1}{2}C_{ijkl}\varepsilon_{ij}\varepsilon_{kl} - e_{ijk}\varepsilon_{ij}E_k - \beta_{ij}\varepsilon_{ij}\phi \\ &\quad - \frac{1}{2}\chi_{kl}E_kE_l - p_kE_k\phi - \frac{\rho c_v}{2\phi_0}\phi^2 \end{aligned} \tag{1}$$

denominated the Gibbs free energy functional, or the enthalpy functional, where η is the enthalpy, C_{ijkl} are elastic moduli, e_{ijk} are the piezoelectric moduli or, more precisely, the constants of piezoelectric deformation, χ_{ij} are dielectric constants, p_k are the pyroelectric

constants, β_{ij} are thermal expansion coefficients, c_v is the specific heat at constant volume, by unit mass, and θ_0 is the reference temperature. Differentiation of this functional with respect to the fields $\boldsymbol{\varepsilon}$, $\boldsymbol{E}$ and θ results in the coupled constitutive relations for a deformable pyro-piezoelectric material, as can be seen in [20].

The formulation utilized in the present paper ignores variations in temperature, such that the coupled equations become

$$\begin{aligned} \sigma_i &= C_{ij}^{E}\varepsilon_j - e_{ik}E_k \\ D_k &= e_{kj}\varepsilon_j + \chi_{kl}^{\varepsilon}E_l \\ \eta &= \beta_j\varepsilon_j + p_kE_k \end{aligned} \tag{2}$$

where σ_{ij} are the components of the mechanical stress tensor, D_i are the components of the electric displacement vector and η is the enthalpy. In (2) the contracted notation was used, considering the stress and strain tensors to be symmetrical. The enthalpy becomes uncoupled from the other fields, and the problem solution is obtained from the first two equations. These relations can be reordered into one single-matrix linear relation, electromechanically coupled, in the orthotropic material directions, along axes 1, 2 and 3

$$\left\{\begin{matrix}\boldsymbol{\sigma}^1\\ \mathbf{D}^1\end{matrix}\right\}^k = \begin{bmatrix}\mathbf{C}^1 & -\mathbf{e}^{1^T}\\ \mathbf{e}^1 & \boldsymbol{\chi}^1\end{bmatrix}^k \left\{\begin{matrix}\boldsymbol{\varepsilon}^1\\ \mathbf{E}^1\end{matrix}\right\}^k \tag{3}$$

The superscript 1 indicates the coordinate system and k is the number of an arbitrary piezoelectric layer. For the piezoelectric extensional mode of actuation, only the following coefficients in (3) are different to zero: $C_{11}^1, C_{12}^1, C_{13}^1, C_{22}^1, C_{23}^1$, $C_{33}^1, C_{44}^1, C_{55}^1$ and C_{66}^1, for the stiffness matrix; $e_{15}^1, e_{24}^1, e_{31}^1, e_{32}^1$ and e_{33}^1, for the piezoelectric matrix; and χ_{11}^1, χ_{22}^1 and χ_{33}^1 for the dielectric matrix.

In this formulation each composite layer is considered orthotropic, whether it is piezoelectric or not. Therefore, the constitutive relation (3) must be rotated to the global laminate coordinate system, according to the layer orientation angle, and then be combined into the laminate constitutive relation.

In addition, for simple monolithic piezoelectric materials polarized along the principal transverse direction 3 , the piezoelectric properties would be the same in both 1 and 2 in-plane directions. The two piezoelectric constants that are usually tabulated are d_{31} and d_{33} (in the strain formulation) where the first subscript indicates the direction of the electric field and the second subscript the direction of the strain. It can be shown that the material parameters are interrelated by $d_{mi} = e_{ml}C_{li}$.

4. Kinematic hypotheses

In the present study the mechanical bending behavior of the plate is described by the Equivalent Single Layer (ESL) methodology, using the kinematical hypothesis following the *Levinson's* Higher-Order Shear Deformation Theory (HSDT) [21], which can be summarized by the following assumed displacement field

$$\begin{aligned} u(\mathbf{x},t) &= u^0 + z\psi_x + z^3\psi_{3x} \\ v(\mathbf{x},t) &= v^0 + z\psi_y + z^3\psi_{3y} \\ w(\mathbf{x},t) &= w^0 \end{aligned} \tag{4}$$

where (u, v, w) are the Cartesian displacement components. Using the linear strain–displacement relations it is possible to obtain the strain field, which is split into *coplanar strains* $\boldsymbol{\varepsilon}_{mf}(\mathbf{x},t) = \{\varepsilon_x, \varepsilon_y, \gamma_{xy}\}^T$ and *transverse strains* $\boldsymbol{\gamma}_c(\mathbf{x},t) = \{\gamma_{yz}, \gamma_{xz}\}^T$. The coplanar strains are expressed as

$$\boldsymbol{\varepsilon}_{mf}(\mathbf{x},t) = \boldsymbol{\varepsilon}^0 + z\boldsymbol{\kappa}_1 + z^3\boldsymbol{\kappa}_3 \tag{5}$$

where it is possible to identify the *generalized extensional strains*, $\boldsymbol{\varepsilon}^0$, the *generalized flexural rotations*, $\boldsymbol{\kappa}_1$, and the *generalized warp rotations*, $\boldsymbol{\kappa}_3$.

The *transverse shear strains* $\boldsymbol{\gamma}_c(\mathbf{x},t)$ are given by

$$\boldsymbol{\gamma}_c = \boldsymbol{\gamma}^0 + 3z^2\boldsymbol{\kappa}_2 \tag{6}$$

where it is possible to identify the *generalized shear strains*, $\boldsymbol{\gamma}^0$, and the *generalized shear-warp strains*, $\boldsymbol{\kappa}_2$.

It is assumed that the electric potential in an intermediary position z, within an arbitrary piezoelectric layer k, is given by the linear expression

$$\varphi^{(k)}(z) = \frac{z_k - z}{h_k}\varphi_{k-1} \tag{7}$$

where φ_{k-1} is the electric potential value on the lower surface of a piezoelectric layer, and h_k and z_k are the thickness and coordinate of the upper surface of the k-layer, respectively. Throughout this paper, it is assumed that the potential at the upper surface of all piezoelectric layers is zero, i.e., $\varphi_k = 0$.

The electric field is the gradient of the electric potential

$$\mathbf{E}^{(k)} = -\nabla\varphi^{(k)}(z) \tag{8}$$

Therefore, the in-plane components of the electric field, E_x and E_y, are approximated by a linear piecewise function in z and the transverse component E_z is a constant value in z, such that

$$\left\{\begin{matrix}E_x\\ E_y\end{matrix}\right\}^{(k)} = \left(\frac{z - z_k}{h_k}\right)\left\{\begin{matrix}\varphi_{k-1,x}\\ \varphi_{k-1,y}\end{matrix}\right\} = \left(\frac{z - z_k}{h_k}\right)\mathbf{E}_p^{(k)} \tag{9}$$

$$E_z^{(k)} = \frac{\varphi_{k-1}}{h_k} \tag{10}$$

5. Principle of Virtual Work

The statement of the virtual work balance for the electromechanical coupled problem is

$$\begin{aligned} \int_V \boldsymbol{\sigma}^T\delta\boldsymbol{\varepsilon}\,dV - \int_V \mathbf{D}^T\delta\mathbf{E}\,dV = &\int_V \overline{\mathbf{F}}^T\delta\mathbf{u}\,dV + \int_{S_\sigma}\overline{\mathbf{T}}^T\delta\mathbf{u}\,dS \\ &+ \int_V \overline{Q}_e\delta\varphi\,dV - \int_{S_q}\bar{q}_e\delta\varphi\,dS \end{aligned} \tag{11}$$

which must be satisfied for any kinematically admissible $\delta\mathbf{u}$ and $\delta\varphi$. The balance stated by (11) is a necessary and sufficient condition to satisfy the local mechanical and electric equilibrium conditions.

Next, standard operations are performed in (11): variations of the generalized deformations are obtained from (5) and (6) and incorporated into the equation. The volume integrals are separated into area and thickness parts, and the z dependencies are explicitly integrated. The resulting expression are obtained in terms of mechanical and electrical resultant generalized forces.

The generalized resultant internal forces are defined as

$$\{\mathbf{N}, \mathbf{M}, \mathbf{M}_3\} = \sum_{k=1}^{N}\int_{z_{k-1}}^{z_k}\boldsymbol{\sigma}^{(k)}\,\{1, z, z^3\}dz \tag{12}$$

$$\{\mathbf{Q}, \mathbf{Q}_2\} = \sum_{k=1}^{N}\int_{z_{k-1}}^{z_k}\boldsymbol{\tau}^{(k)}\,\{1, z^2\}dz \tag{13}$$

$$\mathbf{L}^{(k)} = \left\{\begin{matrix}L_x\\ L_y\end{matrix}\right\}^{(k)} = \int_{z_{k-1}}^{z_k}\left(\frac{z - z_k}{h_k}\right)\left\{\begin{matrix}D_x\\ D_y\end{matrix}\right\}^{(k)}dz \tag{14}$$

$$J_k = \int_{z_{k-1}}^{z_k}\frac{D_z^{(k)}}{h_k}dz \tag{15}$$

where $\mathbf{N} = \{N_x,\ N_y,\ N_{xy}\}^T$, $\mathbf{M} = \{M_x,\ M_y,\ M_{xy}\}^T$ and $\mathbf{M}_3 = \{M_{3x},\ M_{3y},\ M_{3xy}\}^T$ are in-plane stress resultants, whereas $\mathbf{Q} = \{Q_y,\ Q_x\}^T$ and $\mathbf{Q}_2 = \{Q_{2y},\ Q_{2x}\}^T$ are transverse shear stress resultants, and $\boldsymbol{\sigma} = \{\sigma_x,\ \sigma_y,\ \tau_{xy}\}^T$ and $\boldsymbol{\tau} = \{\tau_{yz},\ \tau_{xz}\}^T$. It is important to note that both $\mathbf{L}^{(k)}$, the in-plane electrical displacement resultant, and J_k, the transversal electrical displacement resultant, are defined for each piezoelectric layer.

In the derivation of the virtual work done by the external forces, the body is considered to be subjected to distributed forces on the upper surface $\{\bar{q}_{sx},\ \bar{q}_{sy},\ \bar{q}_{sz}\}$, on the lower surface $\{\bar{q}_{ix},\ \bar{q}_{iy},\ \bar{q}_{iz}\}$ and on the boundary $\{\overline{T}_n,\ \overline{T}_{ns},\ \overline{T}_{nz}\}$. $\overline{T}_n$, $\overline{T}_{ns}$ and $\overline{T}_{nz}$ are the normal, in-plane and transverse shear forces per unity area, respectively. Here, $n$and s are the normal and tangential directions at the boundary, respectively, which are used to express resultant forces and generalized displacement at an arbitrary point of the boundary.

It is assumed that the volumetric free charge is zero, that is, $\overline{Q}_e = 0$, since the piezoelectric material is dielectric and does not contain free electric charge. Also, in this work the application of a surface free electric charge, denoted by $\bar{q}_{ek}$, is assumed only on the lower surface of a piezoelectric layer k. The upper surface of each layer is assumed to be free of charge. Additionally, it is important to note that $\delta\varphi$ is null on the upper surface of each piezoelectric layer, such that only the lower surface contributes to the virtual work in the last integral in Eq. (11).

The following generalized external forces on the bi-dimensional domain are defined

$$\begin{Bmatrix} \bar{q}_x \\ \bar{q}_y \\ \bar{q}_z \end{Bmatrix} = \begin{Bmatrix} \bar{q}_{sx} + \bar{q}_{ix} \\ \bar{q}_{sy} + \bar{q}_{iy} \\ \bar{q}_{sz} + \bar{q}_{iz} \end{Bmatrix} + \int_{-h/2}^{h/2} \begin{Bmatrix} F_x \\ F_y \\ F_z \end{Bmatrix} dz$$
$$\begin{Bmatrix} \bar{m}_x \\ \bar{m}_y \end{Bmatrix} = \frac{h}{2} \begin{Bmatrix} \bar{q}_{iy} - \bar{q}_{sy} \\ \bar{q}_{sx} - \bar{q}_{ix} \end{Bmatrix} + \int_{-h/2}^{h/2} z \begin{Bmatrix} -F_y \\ F_x \end{Bmatrix} dz \tag{16}$$
$$\begin{Bmatrix} \bar{m}_{3x} \\ \bar{m}_{3y} \end{Bmatrix} = \frac{h^3}{8} \begin{Bmatrix} \bar{q}_{iy} - \bar{q}_{sy} \\ \bar{q}_{sx} - \bar{q}_{ix} \end{Bmatrix} + \int_{-h/2}^{h/2} z^3 \begin{Bmatrix} -F_y \\ F_x \end{Bmatrix} dz$$

Moreover, the generalized external forces applied on the boundary are

$$\begin{bmatrix} \overline{N}_n & \overline{M}_n \\ \overline{N}_{ns} & \overline{M}_{ns} \\ \overline{Q}_n & \overline{M}_{3n} \\ & \overline{M}_{3ns} \end{bmatrix} = \int_{-h/2}^{h/2} \begin{bmatrix} \overline{T}_n & z\overline{T}_n \\ \overline{T}_{ns} & z\overline{T}_{ns} \\ \overline{T}_{nz} & z^3\overline{T}_n \\ & z^3\overline{T}_{ns} \end{bmatrix} dz \tag{17}$$

and the generalized inertial forces are

$$\begin{aligned} f_x &= \ddot{u}^0\rho_0 + \ddot{\psi}_x\rho_1 + \ddot{\psi}_{3x}\rho_3 \\ f_y &= \ddot{v}^0\rho_0 + \ddot{\psi}_y\rho_1 + \ddot{\psi}_{3y}\rho_3 \\ f_z &= \ddot{w}^0\rho_0 \\ f_{mx} &= \ddot{u}^0\rho_1 + \ddot{\psi}_x\rho_2 + \ddot{\psi}_{3x}\rho_4 \\ f_{my} &= \ddot{v}^0\rho_1 + \ddot{\psi}_y\rho_2 + \ddot{\psi}_{3y}\rho_4 \\ f_{3mx} &= \ddot{u}^0\rho_3 + \ddot{\psi}_x\rho_4 + \ddot{\psi}_{3x}\rho_6 \\ f_{3my} &= \ddot{v}^0\rho_3 + \ddot{\psi}_y\rho_4 + \ddot{\psi}_{3y}\rho_6 \end{aligned} \tag{18}$$

where the generalized mass moments are defined as

$$\rho_j = \sum_{k=1}^{N} \int_{z_{k-1}}^{z_k} \rho^{(k)}\ z^j\, dz, \quad j = 0, 1, 2, 3, 4, 6 \tag{19}$$

The variations of generalized deformations are substituted by variations of generalized displacements, and integration by parts is preformed on the area integrals. Following standard procedures of variational calculus, the local equilibrium equations in terms of resultant forces are obtained as

$$\begin{aligned} &\frac{\partial N_x}{\partial x} + \frac{\partial N_{xy}}{\partial y} + \bar{q}_x = f_x \\ &\frac{\partial N_{xy}}{\partial x} + \frac{\partial N_y}{\partial y} + \bar{q}_y = f_y \\ &\frac{\partial Q_x}{\partial x} + \frac{\partial Q_y}{\partial y} + \bar{q}_z = f_z \\ &\frac{\partial M_x}{\partial x} + \frac{\partial M_{xy}}{\partial y} - Q_x + \bar{m}_y = f_{mx} \\ &\frac{\partial M_{xy}}{\partial x} + \frac{\partial M_y}{\partial y} - Q_y - \overline{m}_x = f_{my} \\ &\frac{\partial M_{3x}}{\partial x} + \frac{\partial M_{3xy}}{\partial y} - 3Q_{2x} + \overline{m}_{3y} = f_{3mx} \\ &\frac{\partial M_{3xy}}{\partial x} + \frac{\partial M_{3y}}{\partial y} - 3Q_{2y} - \overline{m}_{3x} = f_{3my} \\ &\frac{\partial L_x^{(k)}}{\partial x} + \frac{\partial L_y^{(k)}}{\partial y} - J_k + \bar{q}_{ek} = 0 \end{aligned} \tag{20}$$

The following variational consistent boundary conditions are also obtained

$$\begin{aligned} &N_n = \overline{N}_n \quad M_n = \overline{M}_n \quad M_{3n} = \overline{M}_{3n} \\ &N_{ns} = \overline{N}_{ns} \quad M_{ns} = \overline{M}_{ns} \quad M_{3ns} = \overline{M}_{3ns} \quad Q_n = \overline{Q}_n \end{aligned} \tag{21}$$

on Γ_σ, the portion of the reference surface boundary where external loads are applied, and $L_n^{(k)} = 0$ on $\Gamma_q^{(k)}$ of the lower surface of each piezoelectric layer k. The forces on a curved boundary are given by

$$\begin{Bmatrix} N_n \\ N_{ns} \end{Bmatrix} = \begin{bmatrix} n_x^2 & n_y^2 & 2n_xn_y \\ -n_xn_y & n_xn_y & n_x^2 - n_y^2 \end{bmatrix} \begin{Bmatrix} N_x \\ N_y \\ N_{xy} \end{Bmatrix} \tag{22}$$

Relations for M_n, M_{ns}, M_{3n} and M_{3ns} are analogous to those for N_n and N_{ns}. In addition

$$\begin{aligned} Q_n &= Q_xn_x + Q_yn_y \\ L_n^{(k)} &= L_x^{(k)}n_x + L_y^{(k)}n_y \end{aligned} \tag{23}$$

If there is a free electric charge distributed on the piezoelectric surface, one has the boundary condition $L_n^{(k)} = \overline{L}_m^{(k)}$.

6. Constitutive equations of the piezoelectric laminate

The constitutive equations of a laminate relate the generalized internal forces to the generalized strains and each layer is assumed to consist of an orthotropic or transversally isotropic material.

An important aspect is an inherent limitation related to the HSDT model used here because σ_3^x is assumed to vanish. Hence, similarly to the correction proposed by [22] for their model based on the FSDT, the imposition of the condition $\sigma_3^x = 0$ with the elimination of ε_3^x leads to modified coefficients of the constitutive matrices as

$$\begin{aligned} &C_{11} = \overline{C}_{11} - \frac{(\overline{C}_{13})^2}{\overline{C}_{33}} \qquad C_{12} = \overline{C}_{12} - \frac{\overline{C}_{13}\overline{C}_{23}}{\overline{C}_{33}} \\ &C_{16} = \overline{C}_{16} - \frac{\overline{C}_{13}\overline{C}_{36}}{\overline{C}_{33}} \qquad C_{22} = \overline{C}_{22} - \frac{(\overline{C}_{23})^2}{\overline{C}_{33}} \\ &C_{26} = \overline{C}_{26} - \frac{\overline{C}_{23}\overline{C}_{36}}{\overline{C}_{33}} \qquad C_{66} = \overline{C}_{66} - \frac{(\overline{C}_{36})^2}{\overline{C}_{33}} \\ &C_{44} = \overline{C}_{44} \qquad C_{45} = \overline{C}_{45} \qquad C_{55} = \overline{C}_{55} \\ &e_{14} = \overline{e}_{14} \qquad e_{15} = \overline{e}_{15} \qquad e_{24} = \overline{e}_{24} \qquad e_{25} = \overline{e}_{25} \\ &e_{31} = \overline{e}_{31} + \frac{\overline{C}_{13}\overline{e}_{33}}{\overline{C}_{33}} \quad e_{32} = \overline{e}_{32} + \frac{\overline{C}_{23}\overline{e}_{33}}{\overline{C}_{33}} \quad e_{36} = \overline{e}_{36} + \frac{\overline{e}_{33}\overline{C}_{36}}{\overline{C}_{33}} \\ &\chi_{11} = \overline{\chi}_{11} \quad \chi_{12} = \overline{\chi}_{12} \quad \chi_{22} = \overline{\chi}_{22} \quad \chi_{33} = \overline{\chi}_{33} + \frac{(\overline{e}_{33})^2}{\overline{C}_{33}} \end{aligned} \tag{24}$$

where the barred quantities $\bar{\bullet}$ are the coefficients obtained from the property matrices after axis rotation.

Therefore, using the definitions of the resultant internal forces, (12)–(15), the strain–displacement relations, (5) and (6), the potential–electric field relations, (9) and (10), and the constitutive equations, partitioned into in-plane stresses and transversal shear stresses as well as in-plane electric displacement and transversal electric displacement, for an arbitrary layer k, it is possible to define the laminate constitutive equations, which involve the generalized internal resultant forces and the generalized strains

$$\mathbf{N} = \mathbf{A}\boldsymbol{\varepsilon}^0 + \mathbf{B}\boldsymbol{\kappa}_1 + \mathbf{L}\boldsymbol{\kappa}_3 - \sum_{k=1}^{n_{piez}} \mathbf{e}_{mf}^{(k)^T}\ \varphi_{k-1} \tag{25}$$

$$\mathbf{M} = \mathbf{B}\boldsymbol{\varepsilon}^0 + \mathbf{D}\boldsymbol{\kappa}_1 + \mathbf{F}\boldsymbol{\kappa}_3 - \sum_{k=1}^{n_{piez}} \mathbf{e}_{mf}^{(k)^T}\ \varphi_{k-1}\bar{z}_{1,k} \tag{26}$$

$$\mathbf{M}_3 = \mathbf{L}\boldsymbol{\varepsilon}^0 + \mathbf{F}\boldsymbol{\kappa}_1 + \mathbf{H}\boldsymbol{\kappa}_3 - \sum_{k=1}^{n_{piez}} \mathbf{e}_{mf}^{(k)^T}\ \varphi_{k-1}\bar{z}_{2,k} \tag{27}$$

$$\mathbf{Q} = \mathbf{A}^{\mathbf{c}}\boldsymbol{\gamma}^0 + \boldsymbol{D}^{\mathbf{c}}\boldsymbol{\kappa}_2 + \sum_{k=1}^{n_{piez}} \mathbf{e}_c^{(k)^T}\bar{z}_{1,k}\begin{Bmatrix}\varphi_{k-1,x}\\ \varphi_{k-1,y}\end{Bmatrix}^{(k)} \tag{28}$$

$$\mathbf{Q}_2 = \mathbf{D}^{\mathbf{c}}\boldsymbol{\gamma}^0 + \boldsymbol{F}^{\mathbf{c}}\boldsymbol{\kappa}_2 + \sum_{k=1}^{n_{piez}} \mathbf{e}_c^{(k)^T}\bar{z}_{3,k}\begin{Bmatrix}\varphi_{k-1,x}\\ \varphi_{k-1,y}\end{Bmatrix}^{(k)} \tag{29}$$

$$L^{(k)} = -\frac{h_k}{2}\mathbf{e}_c^{(k)}\gamma_0 - \bar{z}_{3,k}\mathbf{e}_c^{(k)}3\boldsymbol{\kappa}_2 + \bar{z}_{4,k}\boldsymbol{\chi}_c^{(k)}\begin{Bmatrix}\varphi_{k-1,x}\\ \varphi_{k-1,y}\end{Bmatrix} \tag{30}$$

$$J_k = \mathbf{e}_{mf}^{(k)}\cdot\boldsymbol{\varepsilon}^0 + \bar{z}_{1,k}\mathbf{e}_{mf}^{(k)}\cdot\boldsymbol{\kappa}_1 + \bar{z}_{2,k}\mathbf{e}_{mf}^{(k)}\cdot\boldsymbol{\kappa}_3 + \frac{\chi_{33}^{(k)}}{h_k}\varphi_{k-1} \tag{31}$$

with

$$\begin{aligned}
&\bar{z}_{1,k} = \frac{1}{2h_k}(z_k^2 - z_{k-1}^2) \qquad \bar{z}_{2,k} = \frac{1}{4h_k}(z_k^4 - z_{k-1}^4)\\
&\bar{z}_{3,k} = \frac{1}{h_k}\left(\frac{z_k^4}{12} - \frac{z_k z_{k-1}^3}{3} + \frac{z_{k-1}^4}{4}\right)\\
&\bar{z}_{4,k} = \frac{1}{h_k^2}\left(\frac{z_k^3}{3} + z_k z_{k-1}^2 - z_k^2 z_{k-1} - \frac{z_{k-1}^3}{3}\right)
\end{aligned} \tag{32}$$

The sub-matrices **A**, **B**, **D**, **F**, **H** and **L** are components of the *purely mechanical constitutive matrix of membrane and bending of the laminate*, of dimensions 9×9, and the sub-matrices $\mathbf{A}^{\mathbf{c}}$, $\mathbf{D}^{\mathbf{c}}$, $\mathbf{F}^{\mathbf{c}}$, are the components of the *purely mechanical constitutive matrix of transverse shear of the laminate*, of dimensions 4×4. Their components are obtained by integration along the thickness in the following way

$$\begin{Bmatrix}A_{ij}\\ B_{ij}\\ D_{ij}\\ L_{ij}\\ F_{ij}\\ H_{ij}\end{Bmatrix} = \sum_{k=1}^{N}\int_{z_{k-1}}^{z_k} C_{ij}^k \begin{Bmatrix}1\\ z\\ z^2\\ z^3\\ z^4\\ z^6\end{Bmatrix} dz, \quad i,j = 1,2,6 \tag{33}$$

$$\begin{Bmatrix}A_{ij}^c\\ D_{ij}^c\\ F_{ij}^c\end{Bmatrix} = \sum_{k=1}^{N}\int_{z_{k-1}}^{z_k} C_{ij}^k \begin{Bmatrix}1\\ z^2\\ z^4\end{Bmatrix} dz, \quad i,j = 4,5 \tag{34}$$

Moreover, we have the definitions

$$\begin{aligned}
&\mathbf{e}_{mf}^{(k)} = \{\, e_{31} \quad e_{32} \quad e_{36}\,\}^{(k)}\\
&\mathbf{e}_c^{(k)} = \begin{bmatrix}e_{14} & e_{15}\\ e_{24} & e_{25}\end{bmatrix}^{(k)} \qquad \boldsymbol{\chi}_c^{(k)} = \begin{bmatrix}\chi_{11} & \chi_{12}\\ \chi_{12} & \chi_{22}\end{bmatrix}^{(k)}
\end{aligned} \tag{35}$$

7. Equations of motion in terms of generalized displacements

The strain–displacement relations (5), (6), (9) and (10) are substituted in the constitutive relations of the laminate, Eqs. (25)–(31). Next, the generalized internal resultant forces in these equations are substituted in (20), which results in the motion equations in terms of the generalized displacements

$$\begin{aligned}
&A_{11}\frac{\partial^2 u^0}{\partial x^2} + 2A_{16}\frac{\partial^2 u^0}{\partial x\partial y} + A_{66}\frac{\partial^2 u^0}{\partial y^2} + A_{16}\frac{\partial^2 v^0}{\partial x^2} + (A_{12}+A_{66})\frac{\partial^2 v^0}{\partial x\partial y}\\
&+ A_{26}\frac{\partial^2 v^0}{\partial y} + B_{11}\frac{\partial^2\psi_x}{\partial x^2} + 2B_{16}\frac{\partial^2\psi_x}{\partial x\partial y} + B_{66}\frac{\partial^2\psi_x}{\partial y^2} + B_{16}\frac{\partial^2\psi_y}{\partial x^2}\\
&+ (B_{12}+B_{66})\frac{\partial^2\psi_y}{\partial x\partial y} + B_{26}\frac{\partial^2\psi_y}{\partial y^2} + L_{11}\frac{\partial^2\psi_{3x}}{\partial x^2} + 2L_{16}\frac{\partial^2\psi_{3x}}{\partial x\partial y}\\
&+ L_{66}\frac{\partial^2\psi_{3x}}{\partial y^2} + L_{16}\frac{\partial^2\psi_{3y}}{\partial x^2} + (L_{12}+L_{66})\frac{\partial^2\psi_{3y}}{\partial x\partial y} + L_{26}\frac{\partial^2\psi_{3y}}{\partial y^2}\\
&- \sum_{k=1}^{n_{piez}} e_{31}^{(k)}\frac{\partial\varphi_{k-1}}{\partial x} - \sum_{k=1}^{n_{piez}} e_{36}^{(k)}\frac{\partial\varphi_{k-1}}{\partial y} + \bar{q}_x = f_x
\end{aligned} \tag{36}$$

$$\begin{aligned}
&A_{16}\frac{\partial^2 u^0}{\partial x^2} + (A_{12}+A_{66})\frac{\partial^2 u^0}{\partial x\partial y} + A_{26}\frac{\partial^2 u^0}{\partial y^2} + A_{66}\frac{\partial^2 v^0}{\partial x^2} + 2A_{26}\frac{\partial^2 v^0}{\partial x\partial y}\\
&+ A_{22}\frac{\partial^2 v^0}{\partial y^2} + B_{16}\frac{\partial^2\psi_x}{\partial x^2} + (B_{12}+B_{66})\frac{\partial^2\psi_x}{\partial x\partial y} + B_{26}\frac{\partial^2\psi_x}{\partial y^2}\\
&+ B_{66}\frac{\partial^2\psi_y}{\partial x^2} + 2B_{26}\frac{\partial^2\psi_y}{\partial x\partial y} + B_{22}\frac{\partial^2\psi_y}{\partial y^2} + L_{16}\frac{\partial^2\psi_{3x}}{\partial x^2}\\
&+ (L_{12}+L_{66})\frac{\partial^2\psi_{3x}}{\partial x\partial y} + L_{26}\frac{\partial^2\psi_{3x}}{\partial y^2} + L_{66}\frac{\partial^2\psi_{3y}}{\partial x^2} + 2L_{26}\frac{\partial^2\psi_{3y}}{\partial x\partial y}\\
&+ L_{22}\frac{\partial^2\psi_{3y}}{\partial y^2} - \sum_{k=1}^{n_{piez}} e_{36}^{(k)}\frac{\partial\varphi_{k-1}}{\partial x} - \sum_{k=1}^{n_{piez}} e_{32}^{(k)}\frac{\partial\varphi_{k-1}}{\partial y} + \bar{q}_y = f_y
\end{aligned} \tag{37}$$

$$\begin{aligned}
&A_{55}^c\frac{\partial\psi_x}{\partial x} + A_{45}^c\frac{\partial\psi_x}{\partial y} + A_{45}^c\frac{\partial\psi_y}{\partial x} + A_{44}^c\frac{\partial\psi_y}{\partial y} + A_{55}^c\frac{\partial^2 w^0}{\partial x^2} + 2A_{45}^c\frac{\partial^2 w^0}{\partial x\partial y}\\
&+ A_{44}^c\frac{\partial^2 w^0}{\partial y^2} + 3D_{55}^c\frac{\partial\psi_{3x}}{\partial x} + 3D_{45}^c\frac{\partial\psi_{3x}}{\partial y} + 3D_{44}^c\frac{\partial\psi_{3y}}{\partial y} + 3D_{45}^c\frac{\partial\psi_{3y}}{\partial x}\\
&+ \sum_{k=0}^{n_{piez}} e_{15}^{(k)}\bar{z}_{1,k}\frac{\partial^2\varphi_{k-1}}{\partial x^2} + \sum_{k=0}^{n_{piez}}\left(e_{14}^{(k)}+e_{25}^{(k)}\right)\bar{z}_{1,k}\frac{\partial^2\varphi_{k-1}}{\partial x\partial y}\\
&+ \sum_{k=0}^{n_{piez}} e_{24}^{(k)}\bar{z}_{1,k}\frac{\partial^2\varphi_{k-1}}{\partial y^2} + \bar{q}_z = f_z
\end{aligned} \tag{38}$$

$$\begin{aligned}
&B_{11}\frac{\partial^2 u^0}{\partial x^2} + 2B_{16}\frac{\partial^2 u^0}{\partial x\partial y} + B_{66}\frac{\partial^2 u^0}{\partial y^2} + B_{16}\frac{\partial^2 v^0}{\partial x^2} + (B_{12}+B_{66})\frac{\partial^2 v^0}{\partial x\partial y}\\
&+ B_{26}\frac{\partial^2 v^0}{\partial y^2} + D_{11}\frac{\partial^2\psi_x}{\partial x^2} + 2D_{16}\frac{\partial^2\psi_x}{\partial x\partial y} + D_{66}\frac{\partial^2\psi_x}{\partial y^2} + D_{16}\frac{\partial^2\psi_y}{\partial x^2}\\
&+ (D_{12}+D_{66})\frac{\partial^2\psi_y}{\partial x\partial y} + D_{26}\frac{\partial^2\psi_y}{\partial y^2} + F_{11}\frac{\partial^2\psi_{3x}}{\partial x^2} + 2F_{16}\frac{\partial^2\psi_{3x}}{\partial x\partial y}\\
&+ F_{66}\frac{\partial^2\psi_{3x}}{\partial y^2} + F_{16}\frac{\partial^2\psi_{3y}}{\partial x^2} + (F_{12}+F_{66})\frac{\partial^2\psi_{3y}}{\partial x\partial y} + F_{26}\frac{\partial^2\psi_{3y}}{\partial y^2}\\
&- A_{45}^c\psi_y - A_{45}^c\frac{\partial w^0}{\partial y} - A_{55}^c\psi_x - A_{55}^c\frac{\partial w^0}{\partial x} - 3D_{45}^c\psi_{3y} - 3D_{55}^c\psi_{3x}\\
&- \sum_{k=1}^{n_{piez}}\left(e_{31}^{(k)}+e_{15}^{(k)}\right)\bar{z}_{1,k}\frac{\partial\varphi_{k-1}}{\partial x} - \sum_{k=1}^{n_{piez}}\left(e_{36}^{(k)}+e_{25}^{(k)}\right)\bar{z}_{1,k}\frac{\partial\varphi_{k-1}}{\partial y} + \overline{m}_y = f_{mx}
\end{aligned} \tag{39}$$

$$B_{16}\frac{\partial^2 u^0}{\partial x^2}+(B_{12}+B_{66})\frac{\partial^2 u^0}{\partial x\partial y}+B_{26}\frac{\partial^2 u^0}{\partial y^2}+B_{66}\frac{\partial^2 v^0}{\partial x^2}+2B_{26}\frac{\partial^2 v^0}{\partial x\partial y}+B_{22}\frac{\partial^2 v^0}{\partial y^2}+D_{16}\frac{\partial^2\psi_x}{\partial x^2}+(D_{12}+D_{66})\frac{\partial^2\psi_x}{\partial x\partial y}+D_{26}\frac{\partial^2\psi_x}{\partial y^2}+D_{66}\frac{\partial^2\psi_y}{\partial x^2}+2D_{26}\frac{\partial^2\psi_y}{\partial x\partial y}+D_{22}\frac{\partial^2\psi_y}{\partial y^2}+F_{16}\frac{\partial^2\psi_{3x}}{\partial x^2}+(F_{12}+F_{66})\frac{\partial^2\psi_{3x}}{\partial x\partial y}+F_{26}\frac{\partial^2\psi_{3x}}{\partial y^2}+F_{66}\frac{\partial^2\psi_{3y}}{\partial x^2}+2F_{26}\frac{\partial^2\psi_{3y}}{\partial x\partial y}+F_{22}\frac{\partial^2\psi_{3y}}{\partial y^2}-A^c_{44}\psi_y-A^c_{44}\frac{\partial w^0}{\partial y}-A^c_{45}\psi_x-A^c_{45}\frac{\partial w^0}{\partial x}-3D^c_{44}\psi_{3y}-3D^c_{45}\psi_{3x}-\sum_{k=1}^{n_{piez}}\left(e^{(k)}_{36}+e^{(k)}_{14}\right)\bar{z}_{1,k}\frac{\partial\varphi_{k-1}}{\partial x}-\sum_{k=1}^{n_{piez}}\left(e^{(k)}_{32}+e^{(k)}_{24}\right)\bar{z}_{1,k}\frac{\partial\varphi_{k-1}}{\partial y}-\overline{m}_x=f_{my} \tag{40}$$

$$L_{11}\frac{\partial^2 u^0}{\partial x^2}+2L_{16}\frac{\partial^2 u^0}{\partial x\partial y}+L_{66}\frac{\partial^2 u^0}{\partial y^2}+L_{16}\frac{\partial^2 v^0}{\partial x^2}+(L_{12}+L_{66})\frac{\partial^2 v^0}{\partial x\partial y}+L_{26}\frac{\partial^2 v^0}{\partial y^2}+F_{11}\frac{\partial^2\psi_x}{\partial x^2}+2F_{16}\frac{\partial^2\psi_x}{\partial x\partial y}+F_{66}\frac{\partial^2\psi_x}{\partial y^2}+F_{16}\frac{\partial^2\psi_y}{\partial x^2}+(F_{12}+F_{66})\frac{\partial^2\psi_y}{\partial x\partial y}+F_{26}\frac{\partial^2\psi_y}{\partial y^2}+H_{11}\frac{\partial^2\psi_{3x}}{\partial x^2}+2H_{16}\frac{\partial^2\psi_{3x}}{\partial x\partial y}+H_{66}\frac{\partial^2\psi_{3x}}{\partial y^2}+H_{16}\frac{\partial^2\psi_{3y}}{\partial x^2}+(H_{12}+H_{66})\frac{\partial^2\psi_{3y}}{\partial x\partial y}+H_{26}\frac{\partial^2\psi_{3y}}{\partial y^2}-3D^c_{45}\psi_y-3D^c_{45}\frac{\partial w^0}{\partial y}-3D^c_{55}\psi_x-3D^c_{55}\frac{\partial w^0}{\partial x}-9F^c_{45}\psi_{3y}-9F^c_{55}\psi_{3x}-\sum_{k=1}^{n_{piez}}\bar{z}_{2,k}\left(e^{(k)}_{31}\frac{\partial\varphi_{k-1}}{\partial x}+e^{(k)}_{36}\frac{\partial\varphi_{k-1}}{\partial y}\right)-\sum_{k=1}^{n_{piez}}3\bar{z}_{3,k}\left(e^{(k)}_{15}\frac{\partial\varphi_{k-1}}{\partial x}+e^{(k)}_{25}\frac{\partial\varphi_{k-1}}{\partial y}\right)+\overline{m}_{3y}=f_{3mx} \tag{41}$$

$$L_{16}\frac{\partial^2 u^0}{\partial x^2}+(L_{12}+L_{66})\frac{\partial^2 u^0}{\partial x\partial y}+L_{26}\frac{\partial^2 u^0}{\partial y^2}+L_{66}\frac{\partial^2 v^0}{\partial x^2}+2L_{26}\frac{\partial^2 v^0}{\partial x\partial y}+L_{22}\frac{\partial^2 v^0}{\partial y^2}+F_{16}\frac{\partial^2\psi_x}{\partial x^2}+(F_{12}+F_{66})\frac{\partial^2\psi_x}{\partial x\partial y}+F_{26}\frac{\partial^2\psi_x}{\partial y^2}+F_{66}\frac{\partial^2\psi_y}{\partial x^2}+2F_{26}\frac{\partial^2\psi_y}{\partial x\partial y}+F_{22}\frac{\partial^2\psi_y}{\partial y^2}+H_{16}\frac{\partial^2\psi_{3x}}{\partial x^2}+(H_{12}+H_{66})\frac{\partial^2\psi_{3x}}{\partial x\partial y}+H_{26}\frac{\partial^2\psi_{3x}}{\partial y^2}+H_{66}\frac{\partial^2\psi_{3y}}{\partial x^2}+2H_{26}\frac{\partial^2\psi_{3y}}{\partial x\partial y}+H_{22}\frac{\partial^2\psi_{3y}}{\partial y^2}-3D^c_{44}\psi_y-3D^c_{44}\frac{\partial w^0}{\partial y}-3D^c_{45}\psi_x-3D^c_{45}\frac{\partial w^0}{\partial x}-9F^c_{44}\psi_{3y}-9F^c_{45}\psi_{3x}-\sum_{k=1}^{n_{piez}}\bar{z}_{2,k}\left(e^{(k)}_{36}\frac{\partial\varphi_{k-1}}{\partial x}+e^{(k)}_{32}\frac{\partial\varphi_{k-1}}{\partial y}\right)-\sum_{k=1}^{n_{piez}}\bar{z}_{3,k}\left(3e^{(k)}_{14}\frac{\partial\varphi_{k-1}}{\partial x}+3e^{(k)}_{24}\frac{\partial\varphi_{k-1}}{\partial y}\right)-\overline{m}_{3x}=f_{3my} \tag{42}$$

$$-\frac{h_k}{2}\left(e^{(k)}_{14}\frac{\partial\psi_y}{\partial x}+e^{(k)}_{14}\frac{\partial^2 w^0}{\partial x\partial y}+e^{(k)}_{15}\frac{\partial\psi_x}{\partial x}+e^{(k)}_{15}\frac{\partial^2 w^0}{\partial x^2}+e^{(k)}_{24}\frac{\partial\psi_y}{\partial y}+e^{(k)}_{24}\frac{\partial^2 w^0}{\partial y^2}+e^{(k)}_{25}\frac{\partial\psi_x}{\partial y}+e^{(k)}_{25}\frac{\partial^2 w^0}{\partial x\partial y}\right)-\bar{z}_{3,k}\left(3e^{(k)}_{14}\frac{\partial\psi_{3y}}{\partial x}+3e^{(k)}_{15}\frac{\partial\psi_{3x}}{\partial x}+3e^{(k)}_{24}\frac{\partial\psi_{3y}}{\partial y}+3e^{(k)}_{25}\frac{\partial\psi_{3x}}{\partial y}\right)+\bar{z}_{4,k}\left(\chi^{(k)}_{11}\frac{\partial^2\varphi_{k-1}}{\partial x^2}+2\chi^{(k)}_{12}\frac{\partial^2\varphi_{k-1}}{\partial x\partial y}+\chi^{(k)}_{22}\frac{\partial^2\varphi_{k-1}}{\partial y^2}\right)-\left(e^{(k)}_{31}\frac{\partial u^0}{\partial x}+e^{(k)}_{32}\frac{\partial v^0}{\partial y}+e^{(k)}_{36}\frac{\partial u^0}{\partial y}+e^{(k)}_{36}\frac{\partial v^0}{\partial x}\right)-\bar{z}_{1,k}\left(e^{(k)}_{31}\frac{\partial\psi_x}{\partial x}+e^{(k)}_{32}\frac{\partial\psi_y}{\partial y}+e^{(k)}_{36}\frac{\partial\psi_x}{\partial y}+e^{(k)}_{36}\frac{\partial\psi_y}{\partial x}\right)-\bar{z}_{2,k}\left(e^{k}_{31}\frac{\partial\psi_{3x}}{\partial x}+e^{(k)}_{32}\frac{\partial\psi_{3y}}{\partial y}+e^{(k)}_{36}\frac{\partial\psi_{3x}}{\partial y}+e^{(k)}_{36}\frac{\partial\psi_{3y}}{\partial x}\right)-\frac{\chi^{(k)}_{33}}{h_k}\varphi_{k-1}+\bar{q}_{ek}=0 \tag{43}$$

It should be noted that (43) is applied to each piezoelectric layer.

8. Analytic solutions

Here we consider the development of analytic solutions for the problem of a rectangular laminated plate, of dimensions *a* and *b*, as shown in Fig. 1, simply supported at the four edges, under electric

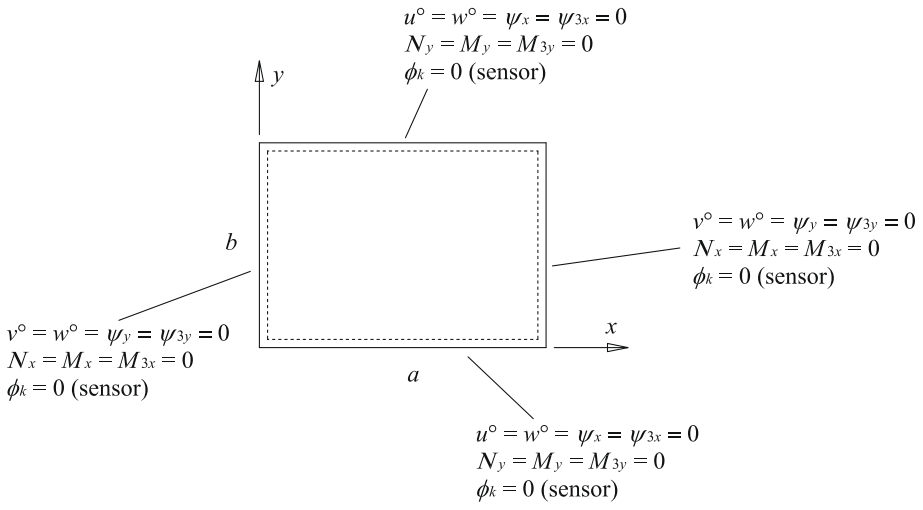

Fig. 1. Simply supported rectangular plate and essential and natural boundary conditions.

and mechanical distributed loads. The essential and natural boundary conditions which must be satisfied are also shown in Fig. 1. The unknown generalized displacements are assumed to be the following infinite trigonometric series in the in-plane directions

$$\begin{Bmatrix} u^0(x,y,t) \\ \psi_x(x,y,t) \\ \psi_{3x}(x,y,t) \end{Bmatrix} = \sum_{m=1}^{\infty}\sum_{n=1}^{\infty} \begin{Bmatrix} U_{mn} \\ X_{mn} \\ \mathbb{X}_{mn} \end{Bmatrix} C_m\, S_n\, e^{i\omega t}$$
$$\begin{Bmatrix} v^0(x,y,t) \\ \psi_y(x,y,t) \\ \psi_{3y}(x,y,t) \end{Bmatrix} = \sum_{m=1}^{\infty}\sum_{n=1}^{\infty} \begin{Bmatrix} V_{mn} \\ Y_{mn} \\ \mathbb{Y}_{mn} \end{Bmatrix} S_m\, C_n\, e^{i\omega t} \tag{44}$$
$$\begin{Bmatrix} w^0(x,y,t) \\ \varphi_{k-1}(x,y,t) \end{Bmatrix} = \sum_{m=1}^{\infty}\sum_{n=1}^{\infty} \begin{Bmatrix} W_{mn} \\ \Phi_{mn}^{(k-1)} \end{Bmatrix} S_m\, S_n\, e^{i\omega t}$$

where $S_m = \sin\alpha_m x$, $S_n = \sin\beta_n y$, $C_m = \cos\alpha_m x$ and $C_n = \cos\beta_n y$, with $\alpha_m = m\pi/a$, $\beta_n = n\pi/b$, m and n are the harmonics, a and b are the dimensions of the plate and ω is the circular frequency.

The equations in (44) satisfy the *natural boundary conditions* under the condition that $A_{16} = A_{26} = B_{16} = B_{26} = D_{16} = D_{26} = L_{16} = L_{26} = F_{16} = F_{26} = H_{16} = H_{26} = 0$.

Moreover, the expansions in Eq. (44) satisfy the equations of motion (36)–(43) under the additional restriction of nullity: $A^c_{45} = D^c_{45} = F^c_{45} = e^{(k)}_{14} = e^{(k)}_{25} = e^{(k)}_{36} = \chi^{(k)}_{12} = 0$.

Therefore, the analytical solution developed next is adequate for square, simply-supported, arbitrary orthotropic base laminates, such as symmetric and antisymmetric cross-ply regular laminates, in which the piezoelectric layers are bonded or embedded.

8.1. Static bending analysis

The static formulation is obtained by setting the frequency to null, $\omega = 0$, in the equations of motion. Next, let us consider transverse mechanical load and electrical distributed load in each layer k, expressed by the following Fourier series

$$\bar{q}_z(x,y) = \sum_{m=1}^{\infty}\sum_{n=1}^{\infty} Q_{mn}\ \text{sen}\ \alpha_m x\ \text{sen}\ \beta_n y$$
$$\bar{q}_{ek}(x,y) = \sum_{m=1}^{\infty}\sum_{n=1}^{\infty} \Theta^{(k)}_{mn}\ \text{sen}\ \alpha_m x\ \text{sen}\ \beta_n y \tag{45}$$

With these expansions for the external loads, the equations of motion are satisfied at all points in the domain, for each given m and n pair, if the algebraic condition, $\mathbf{K}_{mn}\mathbf{Z}_{mn} = \mathbf{F}_{mn}$, is satisfied, where $\mathbf{K}_{mn}$ is the stiffness matrix, symmetric and whose dimension is $n_p \times n_p$, with $n_p = (7 + n_{piez}), \mathbf{Z}_{mn} = \{U_{mn},\ V_{mn},\ W_{mn},\ X_{mn},\ Y_{mn},\ \mathbb{X}_{mn},\ \mathbb{Y}_{mn},\ \Phi^{(1)}_{mn},\ \Phi^{(N_{piez})}_{mn}\}^T$ is the vector of generalized displacements, and $\mathbf{F}_{mn} = \left\{0,\ 0,\ Q_{mn},\ 0,\ 0,\ 0,\ 0,\ \Theta^{(1)}_{mn}\ \Theta^{(N_{piez})}_{mn}\right\}^T$ is the external forces vector, both for a harmonic mn.

The coefficients of $\mathbf{K}_{mn}$ are expressed as follows

$$\begin{aligned}
s_{11} &= A_{11}\alpha_m^2 + A_{66}\beta_n^2 \\
s_{12} &= s_{21} = (A_{12} + A_{66})\alpha_m\beta_n \\
s_{14} &= s_{41} = B_{11}\alpha_m^2 + B_{66}\beta_n^2 \\
s_{15} &= s_{51} = (B_{12} + B_{66})\alpha_m\beta_n \\
s_{16} &= s_{61} = L_{11}\alpha_m^2 + L_{66}\beta_n^2 \\
s_{17} &= s_{71} = (L_{12} + L_{66})\alpha_m\beta_n \\
s_{22} &= A_{66}\alpha_m^2 + A_{22}\beta_n^2 \\
s_{24} &= s_{42} = (B_{12} + B_{66})\alpha_m\beta_n \\
s_{25} &= s_{52} = B_{66}\alpha_m^2 + B_{22}\beta_n^2 \\
s_{26} &= s_{62} = (L_{12} + L_{66})\alpha_m\beta_n \\
s_{27} &= s_{72} = L_{66}\alpha_m^2 + L_{22}\beta_n^2 \\
s_{33} &= A^c_{55}\alpha_m^2 + A^c_{44}\beta_n^2 \\
s_{34} &= s_{43} = A^c_{55}\alpha_m \\
s_{35} &= s_{53} = A^c_{44}\beta_n \\
s_{36} &= s_{63} = 3D^c_{55}\alpha_m \\
s_{37} &= s_{73} = 3D^c_{44}\beta_n \\
s_{44} &= D_{11}\alpha_m^2 + D_{66}\beta_n^2 + A^c_{55} \\
s_{45} &= s_{54} = (D_{12} + D_{66})\alpha_m\beta_n \\
s_{46} &= s_{64} = F_{11}\alpha_m^2 + F_{66}\beta_n^2 + 3D^c_{55} \\
s_{47} &= s_{74} = (F_{12} + F_{66})\alpha_m\beta_n \\
s_{55} &= D_{66}\alpha_m^2 + D_{22}\beta_n^2 + A^c_{44} \\
s_{56} &= s_{65} = (F_{12} + F_{66})\alpha_m\beta_n \\
s_{57} &= s_{75} = F_{66}\alpha_m^2 + F_{22}\beta_n^2 + 3D^c_{44} \\
s_{66} &= H_{11}\alpha_m^2 + H_{66}\beta_n^2 + 9F^c_{55} \\
s_{67} &= s_{76} = (H_{12} + H_{66})\alpha_m\beta_n \\
s_{77} &= H_{66}\alpha_m^2 + H_{22}\beta_n^2 + 9F^c_{44} \\
s_{1(7+k)} &= \alpha_m e^{(k)}_{31} \\
s_{2(7+k)} &= \beta_n e^{(k)}_{32} \\
s_{3(7+k)} &= \frac{h_k}{2}\left(\alpha_m^2 e^{(k)}_{15} + \beta^{(k)}_n e^{2}_{24}\right) \\
s_{4(7+k)} &= \alpha_m\left(\bar{z}_{1,k} e^{(k)}_{31} + \frac{h_k}{2} e^{(k)}_{15}\right) \\
s_{5(7+k)} &= \beta_n\left(\bar{z}_{1,k} e^{(k)}_{32} + \frac{h_k}{2} e^{(k)}_{24}\right) \\
s_{6(7+k)} &= \alpha_m\left(\bar{z}_{2,k} e^{(k)}_{31} + \bar{z}_{3,k} 3e^{(k)}_{15}\right) \\
s_{7(7+k)} &= \beta_n\left(\bar{z}_{2,k} e^{(k)}_{32} + \bar{z}_{3,k} 3e^{(k)}_{24}\right) \\
s_{(7+k)(7+k)} &= -\left[\bar{z}_{4,k}\left(\chi^{(k)}_{11}\alpha_m^2 + \chi^{(k)}_{22}\beta_n^2\right) + \frac{1}{h_k}\chi^{(k)}_{33}\right]
\end{aligned} \tag{46}$$

8.2. Free vibration analysis

The free vibration formulation is obtained zeroing the external forces applied to the motion Eqs. (36)–(43), substituting the generalized displacement expansions (44) and applying the restrictions of nullity to some stiffness coefficients of the laminate, as shown at the beginning of this section. The motion equations are satisfied if the condition $\mathbf{K}\mathbf{Z}_{mn} = \omega^2\mathbf{M}\mathbf{Z}_{mn}$ is satisfied. This is a typical real symmetric eigenvalue problem, where each eigenvector $\mathbf{Z}_{mn}$ is associated with an eigenvalue ω^2. $\mathbf{M}$ is the inertia matrix and its coefficients are defined in (19).

9. Boundary conditions

The final representation of the coupled system can be expressed in matrix form as

$$\begin{bmatrix} \mathbf{M} & \mathbf{0} \\ \mathbf{0} & \mathbf{0} \end{bmatrix} \begin{Bmatrix} \ddot{\mathbf{U}} \\ \ddot{\mathbf{\Phi}} \end{Bmatrix} + \begin{bmatrix} \mathbf{K}_{uu} & \mathbf{K}_{u\phi} \\ \mathbf{K}_{\phi u} & \mathbf{K}_{\phi\phi} \end{bmatrix} \begin{Bmatrix} \mathbf{U} \\ \mathbf{\Phi} \end{Bmatrix} = \begin{Bmatrix} \mathbf{F}(t) \\ \mathbf{Q}(t) \end{Bmatrix} \tag{47}$$

where $\mathbf{K}_{uu}$ is the purely mechanical stiffness matrix, $\mathbf{K}_{u\phi} = \mathbf{K}^T_{\phi u}$ is the piezoelectric stiffness matrix, $\mathbf{K}_{\phi\phi}$ is the purely electrical stiffness matrix, and $\ddot{\bullet}$ stands for the second time derivative. In (47) one can have more than one piezoelectric layer, with $\mathbf{\Phi}$ representing a vector with all electric degrees of freedom and $\mathbf{U}$ contains all mechanical nodal displacements. Here, $\mathbf{F}(t)$ is a vector of generalized forces applied on the reference plane and $\mathbf{Q}(t)$ is the vector of the electric charge on the bottom surfaces of piezoelectric layers.

For purely mechanical essential boundary conditions, it is current practice to partition the mechanical degrees of freedom vector

into prescribed values on the boundary (referred to here as "applied") and free values, that is, $\mathbf{U} = \{\mathbf{U}^f; \mathbf{U}^a\}$, where f stands for free and a stands for applied. Therefore, the appropriate matrices in (47) are also partitioned in the form

$$\begin{bmatrix} \mathbf{M}^{ff} & \mathbf{M}^{fa} & \mathbf{0} \\ \mathbf{M}^{af} & \mathbf{M}^{aa} & \mathbf{0} \\ \mathbf{0} & \mathbf{0} & \mathbf{0} \end{bmatrix} \begin{Bmatrix} \ddot{\mathbf{U}}^f \\ \ddot{\mathbf{U}}^a \\ \ddot{\mathbf{\Phi}} \end{Bmatrix} + \begin{bmatrix} \mathbf{K}_{uu}^{ff} & \mathbf{K}_{uu}^{fa} & \mathbf{K}_{u\phi}^{ff} \\ \mathbf{K}_{uu}^{af} & \mathbf{K}_{uu}^{aa} & \mathbf{K}_{u\phi}^{aa} \\ \mathbf{K}_{\phi u}^{ff} & \mathbf{K}_{\phi u}^{aa} & \mathbf{K}_{\phi\phi} \end{bmatrix} \begin{Bmatrix} \mathbf{U}^f \\ \mathbf{U}^a \\ \mathbf{\Phi} \end{Bmatrix} = \begin{Bmatrix} \mathbf{F} \\ \mathbf{F}_R \\ \mathbf{Q} \end{Bmatrix} \tag{48}$$

Considering system (48) as three matrix equations, the third one is used to isolate $\mathbf{\Phi} = -\mathbf{K}_{\phi\phi}^{-1}[\mathbf{K}_{\phi u}^{aa}\mathbf{U}^a + \mathbf{K}_{\phi u}^{ff}\mathbf{U}^f]$, taking $\mathbf{Q} = \mathbf{0}$ as the sensor case [23]. This expression is used to eliminate $\mathbf{\Phi}$ in the first equation, which generates the reduced algebraic problem (49) for the mechanical unknowns only. This problem is solved first and its solution is used next to obtain $\mathbf{\Phi}$.

$$\mathbf{M}^{ff}\ddot{\mathbf{U}}^f + \overline{\mathbf{K}}\mathbf{U}^f = \overline{\mathbf{F}} \tag{49}$$

with

$$\overline{\mathbf{K}} = \left(\mathbf{K}_{uu}^{ff} - \mathbf{K}_{u\phi}^{ff}(\mathbf{K}_{\phi\phi})^{-1}\mathbf{K}_{\phi u}^{ff}\right) \tag{50}$$

$$\overline{\mathbf{F}} = \mathbf{F} + \left(\mathbf{K}_{u\phi}^{ff}(\mathbf{K}_{\phi\phi})^{-1}\mathbf{K}_{\phi u}^{aa} - \mathbf{K}_{uu}^{fa}\right)\mathbf{U}^a - \mathbf{M}^{fa}\ddot{\mathbf{U}}^a \tag{51}$$

Since the piezoelectric layers may behave as actuators or sensors, the electrical boundary conditions can be imposed by the following procedure, according to [23,24]. The electric potential vector is subdivided into a free or sensory component $\mathbf{\Phi}^f$ representing the voltage output at the sensors, and a forced or active component $\mathbf{\Phi}^a$ representing the voltage imposed on the active layers, such that $\mathbf{\Phi} = \{\mathbf{\Phi}^f; \mathbf{\Phi}^a\}^T$. Thus, the purely electric stiffness $\mathbf{K}_{\phi\phi}$ and coupled piezoelectric matrices $\mathbf{K}_{u\phi}^{fa}$ and $\mathbf{K}_{\phi u}^{fa}$ are partitioned such that

$$\begin{bmatrix} \mathbf{M} & \mathbf{0} & \mathbf{0} \\ \mathbf{0} & \mathbf{0} & \mathbf{0} \\ \mathbf{0} & \mathbf{0} & \mathbf{0} \end{bmatrix} \begin{Bmatrix} \ddot{\mathbf{U}} \\ \ddot{\mathbf{\Phi}}^f \\ \ddot{\mathbf{\Phi}}^a \end{Bmatrix} + \begin{bmatrix} \mathbf{K}_{uu} & \mathbf{K}_{u\phi}^{ff} & \mathbf{K}_{u\phi}^{fa} \\ \mathbf{K}_{\phi u}^{ff} & \mathbf{K}_{\phi\phi}^{ff} & \mathbf{0} \\ \mathbf{K}_{\phi u}^{fa} & \mathbf{0} & \mathbf{K}_{\phi\phi}^{aa} \end{bmatrix} \begin{Bmatrix} \mathbf{U} \\ \mathbf{\Phi}^f \\ \mathbf{\Phi}^a \end{Bmatrix} = \begin{Bmatrix} \mathbf{F} \\ \mathbf{Q}^f \\ \mathbf{Q}^a \end{Bmatrix} \tag{52}$$

The zeroes in the stiffness matrix come from the fact that $\mathbf{K}_{\phi\phi}$ is diagonal due to the layerwise description. Separating the active and sensory potentials, the first two lines of (52) take the following form

$$\begin{bmatrix} \mathbf{M} & \mathbf{0} \\ \mathbf{0} & \mathbf{0} \end{bmatrix} \begin{Bmatrix} \ddot{\mathbf{U}} \\ \ddot{\mathbf{\Phi}}^f \end{Bmatrix} + \begin{bmatrix} \mathbf{K}_{uu} & \mathbf{K}_{u\phi}^{ff} \\ \mathbf{K}_{\phi u}^{ff} & \mathbf{K}_{\phi\phi}^{ff} \end{bmatrix} \begin{Bmatrix} \mathbf{U} \\ \mathbf{\Phi}^f \end{Bmatrix} = \begin{Bmatrix} \mathbf{F} \\ \mathbf{Q}^f \end{Bmatrix} - \begin{Bmatrix} \mathbf{K}_{u\phi}^{fa} \\ \mathbf{0} \end{Bmatrix} \mathbf{\Phi}^a \tag{53}$$

where the right-hand side includes the excitation of the structure in terms of mechanical loads and voltages applied on the actuators. The electric charge at the sensors $\mathbf{Q}^f$ remains constant with time and is assumed to be zero. The second equation in (53) is used to isolate $\mathbf{\Phi}^f$, which is used to eliminate it in the first of the equations in (53). The final system of equations is

$$\begin{cases} \mathbf{M}\ddot{\mathbf{U}} + \overline{\mathbf{K}}\mathbf{U} = \overline{\mathbf{F}} \\ \mathbf{K}_{\phi\phi}^{ff}\mathbf{\Phi}^f = -\mathbf{K}_{\phi u}^{ff}\mathbf{U} \end{cases} \tag{54}$$

with

$$\begin{cases} \overline{\mathbf{K}} = (\mathbf{K}_{uu} - \mathbf{K}_{u\phi}^{ff}(\mathbf{K}_{\phi\phi}^{ff})^{-1}\mathbf{K}_{\phi u}^{ff}) \\ \overline{\mathbf{F}} = \mathbf{F} - \mathbf{K}_{u\phi}^{fa}\mathbf{\Phi}^a \end{cases} \tag{55}$$

The equations in (54) form a set of two uncoupled algebraic problems. The purely mechanical displacements $\mathbf{U}$ are obtained from the first problem and are applied to the right hand side of the second one, whose solution gives the nodal values of the sensory voltages $\mathbf{\Phi}^f$.

10. Numerical results

The first set of applications aims to show the capability of the present formulation to evaluate primal variables, i.e., mechanical displacements and electrical potentials. Such an assessment is accomplished through the static analysis of square homogeneous and composite laminates with piezoelectric layers on the bottom and top surfaces, subjected to distributed mechanical loads or distributed electrical potential. The results are compared with those of an analytical solution based on the LT-FSDT model, developed by Machado [25]. Next, the results for the stress distribution are compared with those of an exact solution based on the elasticity theory presented by Mallik and Ray [10]. Finally, the results for the free vibration analysis of a square piezoelectric composite laminated plate considering two electrical boundary conditions, open and closed circuit, are discussed in Section 9. In all cases, in order to be able to make comparisons with other similar analytical solutions, the host plate is composed of symmetric cross-ply laminates, although the analytical solution is not restricted to this case.

10.1. Case 1 – static bending analysis of homogeneous plate

This case consists of a square plate with three layers. The piezoelectric layers are the first and third ones, and each has a thickness $t/2$, where t is the sum of the thicknesses of all piezoelectric layers. The total laminate thickness is h. The internal layer is assumed be aluminum with the properties $E = 70.0$ GPa and $G = 26.0$ GPa. The piezoelectric layers are PZT, with the following properties

$$E_1 = E_2 = 94.95\ \text{GPa} \quad E_3 = 81.89\ \text{GPa}$$
$$G_{12} = 35.90\ \text{GPa} \quad G_{23} = G_{13} = 25.40\ \text{GPa}$$
$$\nu_{12} = 0.32 \quad \nu_{13} = \nu_{23} = 0.38$$
$$e_{31} = e_{32} = -2.10\ \text{C/m}^2 \quad e_{15} = e_{24} = 9.20\ \text{C/m}^2$$
$$e_{33} = 9.50\ \text{C/m}^2 \quad \chi_{11} = \chi_{22} = 4.07 \times 10^{-9}\ \text{F/m}$$
$$\chi_{33} = 2.08 \times 10^{-9}\ \text{F/m}$$

In the *first load case* the piezoelectric layers are assumed to be sensors, characterizing the *sensitive case*, and a uniformly distributed mechanical load, $q_z(x, y) = 1\ \text{N/m}^2$, is applied. The corresponding Fourier coefficients in (45) are $Q_{mn} = 16/(\pi^2 mn)$, for $m, n = 1, 3, 5, \ldots$.

The *second load case* consists of an *active case*, where a uniformly distributed electrical potential, $\varphi_0 = -\varphi_2 = 1$ V, is applied as the essential boundary conditions on the bottom surfaces of the piezoelectric layers. The corresponding Fourier coefficients in (45) are $\Phi_{mn}^0 = -\Phi_{mn}^2 = 16/(\pi^2 mn)$, for $m, n = 1, 3, 5, \ldots$.

For the sensitive case, the deflections and potentials on the bottom surfaces of the piezoelectric layers are evaluated at the center plate and are shown in Table 1 for several ratios t/h of piezoelectric to laminate thicknesses, and plate aspect ratios a/h of length to laminate thickness. For the active case, the deflections are tabulated in the Table 2.

Table 1 shows that for the sensitive case the results provided by the LT-FSDT [25] and LT-HSDT (this study) agree better for the thicker homogeneous plates. In addition, the relative errors are more expressive for the computed potentials. For the active case, Table 2 shows that there is almost no difference between the two formulations.

10.2. Case 2 – displacement in static bending of composite laminated plates

For the sake of generality and aiming to provide more reference results, a square composite laminated plate is considered with stacking sequence [0/90/0] of Graphite/Epoxy and two PZT-4

Table 1
Maximum deflection and maximum potential for a homogeneous plate with piezoelectric sensors subjected to a uniformly distributed mechanical load.

t/h	Source	a/h					
		$(w/h)\times 10^9$			$(\phi^0/h)\times 10^2$		
		7	10	20	7	10	20
0.10	This study	1.4337	5.6295	86.1268	−3.0078	−6.1127	−24.3769
	[25]	1.4369	5.6299	85.9884	−2.9964	−6.1355	−24.6012
0.20	This study	1.3087	5.1106	77.8483	−5.1104	−10.4197	−41.6509
	[25]	1.3122	5.1092	77.6435	−5.0710	−10.4320	−41.9677
0.30	This study	1.2290	4.7773	72.4956	−6.6806	−13.6755	−54.8219
	[25]	1.2318	4.7732	72.2506	−6.5998	−13.6571	−55.1706
0.40	This study	1.1780	4.5620	69.0151	−7.8958	−16.2431	−65.3446
	[25]	1.1798	4.5552	68.7447	−7.7651	−16.1824	−65.6958

Table 2
Maximum deflection for a homogeneous plate with piezoelectric actuators subjected to distributed uniform electrical potentials.

t/h	Source	$w\times 10^9$		
		a/h		
		7	10	20
0.10	This study	3.5563	7.2201	28.7717
	[25]	3.5511	7.2471	28.9883
0.20	This study	3.1545	6.4117	25.5716
	[25]	3.1553	6.4394	25.7577
0.30	This study	2.8396	5.7750	23.0423
	[25]	2.8426	5.8012	23.2049
0.40	This study	2.5830	5.2439	20.9651
	[25]	2.5858	5.2771	21.1084

piezoelectric layers bonded on the surfaces. The material properties [26] for each substrate layer are

$$E_1 = 132.38\ \text{GPa} \quad E_2 = E_3 = 10.76\ \text{GPa}$$
$$G_{12} = 3.61\ \text{GPa} \quad G_{13} = G_{23} = 5.65\ \text{GPa}$$
$$\nu_{23} = 0.49 \quad \nu_{12} = \nu_{13} = 0.24$$

and the material properties for the PZT-4 are

$$E_1 = E_2 = 81.30\ \text{GPa} \quad E_3 = 64.50\ \text{GPa}$$
$$G_{12} = G_{13} = 25.60\ \text{GPa} \quad G_{23} = 30.60\ \text{GPa}$$
$$\nu_{12} = 0.33 \quad \nu_{13} = \nu_{23} = 0.43$$
$$d_{31} = d_{32} = -122\times 10^{-12}\ \text{C/N} \quad d_{33} = -285\times 10^{-12}\ \text{C/N}$$
$$\chi_{33} = 18.585\times 10^{-9}\ \text{F/m}$$

The plate is subjected to a sinusoidal mechanical load of amplitude $q_z = 1.621\ \text{N/m}^2$ for the sensitive case and to a sinusoidal electrical potential of amplitude $\varphi_0 = -\varphi_4 = 1.621\ \text{V}$, (the layers $k = 1$ and $k = 5$ are piezoelectric), for the active case. The results for maximum deflection and electric potential are given in Tables 3 and 4, respectively. In these tables, the values are normalized to E_2 and d_{32}, which are properties of the base structural layers and the piezoelectric layers, respectively.

10.3. Case 3 – stresses in static bending of composite laminated plates

The performance of the proposed LT-HSDT model to evaluate stress distributions is considered in the problem of a square piezoelectric composite plate subjected to a mechanical load or combined mechanical/electrical loads, as presented by Mallik and Ray [10]. The material properties for the layers of the substrate are

$$E_1 = 172.9\ \text{GPa} \quad E_1/E_2 = E_1/E_3 = 25$$
$$G_{23} = 0.2E_2 \quad G_{12} = G_{13} = 0.5E_2$$
$$\nu_{12} = \nu_{13} = \nu_{23} = 0.25$$

The material properties of the Piezoelectric Fiber Reinforced Composite (PFRC), a composite material obtained by combining an Epoxy matrix with PZT unidirectional fibers, were calculated using the micromechanics model derived by Mallik and Ray [10] and are as follows:

$$C_{11} = 32.6\ \text{GPa} \quad C_{12} = C_{21} = 10.76\ \text{GPa}$$
$$C_{23} = 3.85\ \text{GPa} \quad C_{13} = C_{31} = 4.76\ \text{GPa}$$
$$C_{44} = 1.05\ \text{GPa} \quad C_{22} = C_{33} = 7.20\ \text{GPa}$$
$$C_{55} = C_{66} = 1.29\ \text{GPa} \quad e_{31} = -6.76\ \text{C/m}^2$$
$$\chi_{11} = \chi_{22} = 0.037\times 10^{-9}\ \text{C/Vm} \quad \chi_{33} = 10.64\times 10^{-9}\ \text{C/Vm}$$

Table 3
Maximum deflection and maximum potential for a laminated composite plate with piezoelectric sensors subjected to a sinusoidal mechanical load.

t/h	$(wE_2h^3/a^4q_0)\times 10^3$			$(\phi h^3/q_0 d_{32})\times 10^{-4}$		
	a/h			a/h		
	5	10	20	5	10	20
0.03	13.805	8.816	8.137	1.747	0.368	0.091
0.05	13.021	8.321	7.060	2.638	0.567	0.134
0.10	11.631	7.389	6.263	4.304	0.961	0.231
0.20	10.024	6.248	5.268	6.380	1.494	0.365
0.30	8.934	5.549	4.681	7.662	1.853	0.458
0.40	7.919	5.035	4.300	8.526	2.122	0.529
0.50	6.946	4.631	4.042	9.129	2.336	0.587
0.60	6.122	4.328	3.873	9.555	2.510	0.635
0.70	5.507	4.121	3.771	9.847	2.649	0.674
0.80	5.087	3.995	3.719	10.008	2.755	0.705
0.90	4.816	3.926	3.702	10.021	2.821	0.725
1.00	4.645	3.895	3.705	98.527	2.841	0.735

Table 4
Maximum deflection for a laminated composite plate with piezoelectric actuators subjected to sinusoidal electrical potentials.

t/h	$(wE_2h^3/a^4q_0)\times 10^2$		
	a/h		
	5	10	20
0.03	52.889	22.193	10.437
0.05	48.304	20.689	9.981
0.10	40.022	17.779	8.535
0.20	30.344	14.058	6.858
0.30	24.839	11.773	5.794
0.40	21.298	10.223	5.054
0.50	18.816	9.090	4.504
0.60	16.933	8.205	4.069
0.70	15.392	7.471	3.707
0.80	14.048	6.827	3.388
0.90	12.811	6.233	3.095
1.00	11.621	5.661	2.812

The following non-dimensional parameters are used to present the numerical results

$$(S_x, S_y, S_{xy}) = \frac{1}{f_0 s^2}\left(\sigma_x^k, \sigma_y^k, \tau_{xy}^k\right)$$
$$(S_{xz}, S_{yz}) = \frac{1}{f_0 s}\left(\tau_{xz}^k, \tau_{yz}^k\right) \quad (56)$$

where $s = a/h$ is the length to laminate thickness ratio, and f_0 is the amplitude of the distributed sinusoidal mechanical load. It is important to note that the analytical solution of Mallik and Ray [10] is restricted to a single piezoelectric layer placed on the laminate top surface and, also, the bottom surface of the piezoelectric layer is grounded, i.e., the electric potentials may be different from zero only on the top surface of the piezoelectric layer. In contrast, in the present formulation only the bottom surface of the piezoelectric layer admits non-zero potential. Also, we are able to consider any number of piezoelectric layers. Therefore, in order to represent the loading of Mallik and Ray [10], the present study considers a plate with one piezoelectric layer on the bottom surface, a mechanical load applied upwards and, based on the definition of the electric field vector and the physical effect of the sign of the piezoelectric constants, the positive electrical potential loading here corresponds to a negative electrical potential loading of Mallik and Ray [10].

The substrate is a cross-ply laminate [0/90/0] with all layers having 1 mm of thickness. A single PFRC layer with 250 mm of thickness is bonded onto the bottom surface of the laminate. A distributed sinusoidal mechanical load is applied, of amplitude $f_0 = 40\ \mathrm{N/m^2}$ (upwards), with and without applying voltages of amplitudes 100 V and −100 V to the PFRC.

The comparative results at characteristic points are shown in Table 5, and the stress distributions along the laminate thickness are shown in Figs. 2–6. The transverse shear stresses shown are not those obtained directly from the constitutive relations, but from the post-processing of the local equilibrium equations (see the Appendix A). Therefore, it should be noted that, while all other results displayed are exact with respect to the continuous model, the shear transverse stresses are only approximate results associated with the model. Moreover, in this procedure of integration,

Table 5
Non-dimensional stresses of cross-ply substrates [0/90/0]with and without voltage applied to the PFRC layer.

a/h	V (v)	Source	S_x $(\frac{a}{2}, \frac{b}{2}, \pm\frac{h}{2})$	S_y $(\frac{a}{2}, \frac{b}{2}, \pm\frac{h}{6})$	S_{xy} $(0, 0, \pm\frac{h}{2})$
20	0	This study	−0.4914	−0.1849	0.0210
			0.5312	0.1973	−0.0220
	0	[10]	−0.5035	−0.1901	0.0215
			0.5305	0.2044	−0.0224
	100	This study	−57.1024	−10.6108	1.8334
			19.9104	14.3041	−1.1743
	−100	[10]	−58.276	−10.84	1.8648
			18.875	14.566	−1.1679
	−100	This study	56.1107	10.2393	−1.7912
			−18.8448	−13.9072	1.1300
	100	[10]	57.269	10.459	−1.822
			−17.81	−14.16	1.1232
100	0	This study	−0.4903	−0.1634	0.0196
			0.5181	0.1744	−0.0204
	0	[10]	−0.4948	−0.1643	0.0197
			0.5193	0.1758	−0.0204
	100	This study	−2.7421	−0.5879	0.0921
			1.2585	0.7461	−0.0660
	−100	[10]	−2.7445	−0.5882	0.0922
			1.2566	0.7470	−0.0660
	−100	This study	1.7528	0.2594	−0.0268
			−0.2196	−0.3950	0.0251
	100	[10]	1.7549	0.2596	−0.0527
			−0.2181	−0.3955	0.0251

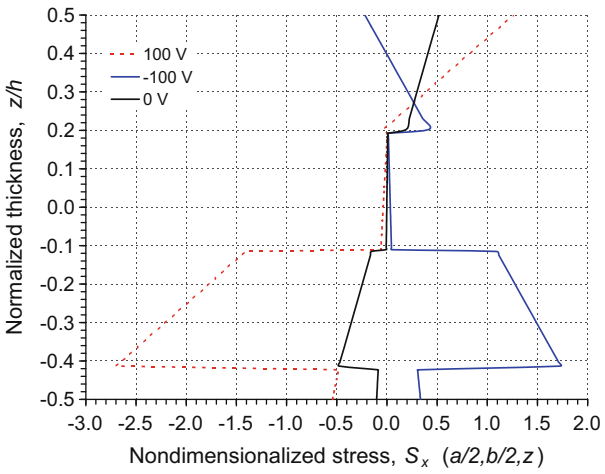

Fig. 2. Distribution of non-dimensional in-plane normal stress for a thin cross-ply laminate with one piezoelectric layer with and without applied voltage.

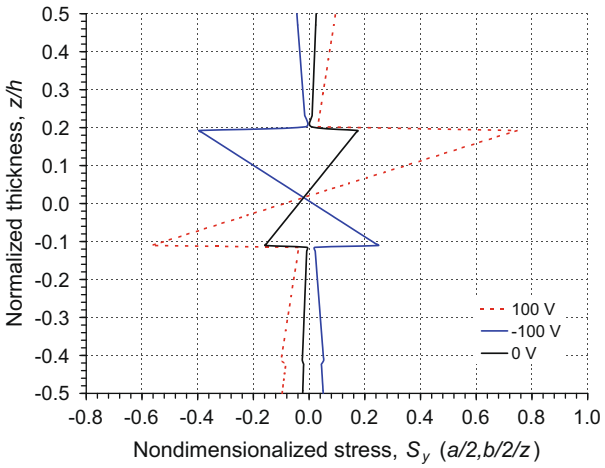

Fig. 3. Distribution of non-dimensional in-plane normal stress for a thin cross-ply laminate with one piezoelectric layer with and without applied voltage.

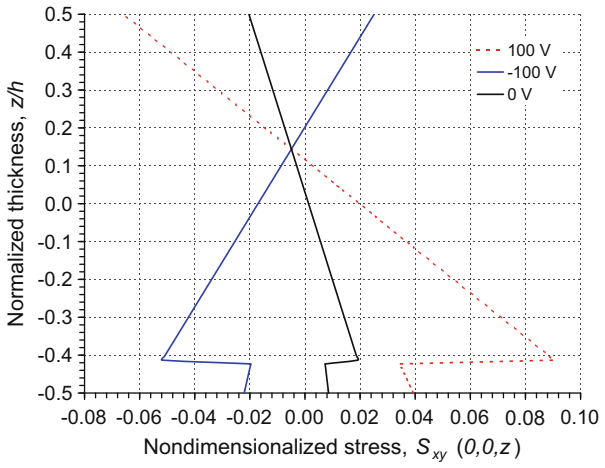

Fig. 4. Distribution of non-dimensional in-plane shear stress for a thin cross-ply laminate with one piezoelectric layer with and without applied voltage.

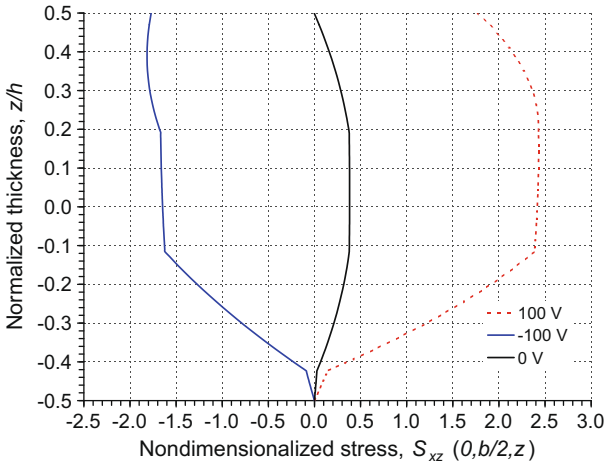

Fig. 5. Distribution of non-dimensional transverse shear stress for a thin cross-ply laminate with one piezoelectric layer with and without applied voltage.

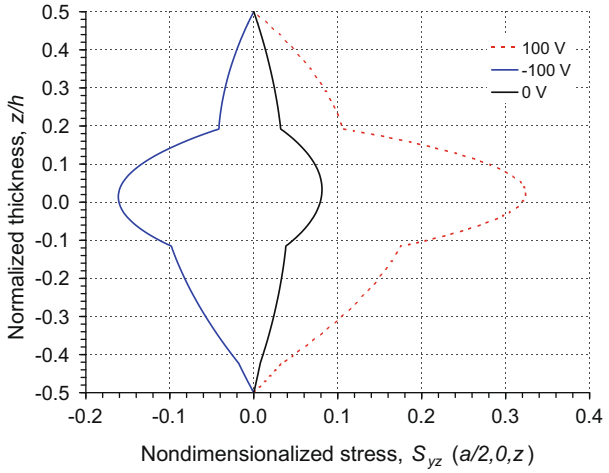

Fig. 6. Distribution of non-dimensional transverse shear stress for a thin cross-ply laminate with one piezoelectric layer with and without applied voltage.

it is only possible to impose the nullity of the transverse shear stresses on the laminate bottom surface. Thus, the implementation used in this study may ensure null transverse shear stresses only on the laminate bottom surface whereas the results displayed by Mallik and Ray [10] show that the transverse shear stresses are null only on the laminate top surface. Therefore, the values for the stress shown in Table 5 at these characteristic points are different, because the stacking sequences are not the same. However, the stress distributions are very similar, as may be seen in Mallik and Ray [10].

The slight difference between the two sets of results is due to the approximation nature of the kinematic model used here with respect to the elasticity solution used in Mallik and Ray [10].

It is possible to note from the figures that the applied voltage changes effectively the response of thin plates. Due the difference of stiffness between the materials, a relatively low applied voltage increases significantly the normal stress S_x in the layer in contact with the activated PFRC layer. Moreover, more severe transverse shear stresses are developed across the thickness. Substantial amount of induced stress can be developed in the structural layers and the reversal takes place due to the change of polarity.

Table 6
Normalized natural frequencies, $a/h = 10$.

t/h	$\bar{\omega}$	
	Closed circuit	Open circuit
0.00	166.19	166.19
0.03	173.92	174.90
0.05	178.51	180.04
0.10	188.46	191.12
0.20	203.73	207.90
0.30	215.46	220.62
0.40	225.62	231.56
0.50	234.75	241.37
0.60	242.44	249.58
0.70	248.24	255.65
0.80	252.16	259.59
0.90	254.61	261.79
1.00	256.10	262.80

Table 7
Normalized natural frequencies, $t/h = 0.20$.

a/h	$\bar{\omega}$	
	Closed circuit	Open circuit
3	119.50	120.79
4	143.21	145.10
5	161.17	163.62
10	203.73	207.89
15	216.79	221.61
20	222.08	227.18
25	224.69	229.93
30	226.15	231.47
35	227.04	232.42
40	227.63	233.04
45	228.04	233.47
50	228.33	233.78

10.4. Case 4 – free vibration analysis of composite laminated plate

The free vibration problem of a five-ply simply supported square laminated composite plate with surface bonded piezoelectric layers is now considered in order to validate the model developed in the evaluation of natural frequencies. The laminate is made of three layers of Graphite/Epoxy with the stacking sequence [0/90/0] and two surface bonded PZT-4 piezoelectric layers. The properties of the materials are the same as those used in Section 10.2, provided by [26], and the value of the first natural frequency, obtained with the finite element method, is taken as a reference since these authors also used a higher-order theory for the displacement field. The density is assumed to be $\rho = 1\ \mathrm{kg/m^3}$ for all layers. The natural frequencies for an open and closed circuit are given in Tables 6 and 7 for several piezoelectric to laminate thickness ratios t/h, and plate aspect ratios a/h of length to laminate thickness. The results are normalized by the parameter $\bar{\omega} = \frac{\omega a^2}{h\sqrt{\rho}} \times 10^3\ \mathrm{Hz(kg/m)}^{1/2}$.

The difference between the results for the two simulated electrical boundary conditions becomes more significant for thin plates, as can be noted in Table 7. In general, the open circuit condition, when the electric potentials are unknown variables, leads to higher first normalized natural frequencies. However, with the expression for the normalized parameter $\overline{\omega}$ in mind, it is possible to note that the closed circuit condition, when the piezoelectric layers are grounded, i.e., the potentials are enforced to be nulls, the stiffness of the plate is increased.

11. Concluding remarks

This paper presents a hybrid plate theory for analysis of piezoelectric laminated composite plates based on a Higher-Order Shear

Deformation Theory and a Layerwise Theory. The HSDT used for the mechanical displacements is a general cubic expansion in the z coordinate with inextensible transverse normal. The Layerwise Theory used for the electric potential admits a linear variation of potential across each piezoelectric layer.

The equilibrium equations in terms of generalized resultant internal forces are obtained from the Principle of Virtual Work and subsequently the equations of motion in terms of generalized displacements and potentials are derived. The formulation is complete in the sense that it takes into account all material coefficients and may be applied to static or dynamic analysis.

Analytic solutions for static problems in sensor and active cases as well as for free vibration are developed for orthotropic square simply-supported laminates with piezoelectric layers.

The proposed model allows piezoelectric layers at any position along the laminate thickness, and in-plane and transverse distributed mechanical forces and electrical loadings can be considered.

Numerical results were obtained for cross-ply laminates and compared to similar models. The results are displayed in table and figures for easy reference.

The kinematical assumptions provided useful representation for bending of cross-ply piezoelectric laminated plates as shown by the assessments of displacements and electric potentials as well as stresses.

Acknowledgements

D.A.F. Torres gratefully acknowledges the financial support provided by the Brazilian government agencies CAPES (Coordenação de Aperfeiçoamento de Pessoal de Nível Superior) and CNPq (Conselho Nacional de Desenvolvimento Científico e Tecnológico) during this research.

Appendix A. Stress computations

The in-plane stresses in each layer k can be computed from $\boldsymbol{\sigma}^k(\mathbf{x},t) = \mathbf{C}^k\boldsymbol{\varepsilon}^k(\mathbf{x},t)$, where

$$\mathbf{C}^k = \begin{bmatrix} C_{11} & C_{12} & C_{16} \\ C_{12} & C_{22} & C_{26} \\ C_{16} & C_{26} & C_{66} \end{bmatrix}^k \tag{57}$$

whose stiffness coefficients are given in (24).

The transverse shear stresses are evaluated by integration of local equilibrium equations, which can be accomplished in each layer as follows (in the absence of body forces)

$$\begin{aligned} \tau_{xz}^{(k)}(\mathbf{x},t) - \tau_{xz}^{(k)}(x,y,z_{k-1},t) &= -\int_{z_{k-1}}^{z} \sigma_{x,x}^{(k)} + \tau_{xy,y}^{(k)}\,dz \\ \tau_{yz}^{(k)}(\mathbf{x},t) - \tau_{yz}^{(k)}(x,y,z_{k-1},t) &= -\int_{z_{k-1}}^{z} \tau_{xy,x}^{(k)} + \sigma_{y,y}^{(k)}\,dz \end{aligned} \tag{58}$$

The stress derivatives for each harmonic are

$$\begin{aligned} \sigma_{x,x} = -\sum_{m=1}^{\infty}\sum_{n=1}^{\infty} \big(&C_{11}\alpha_m^2\overline{U}_{mn}C_mS_n + C_{12}\alpha_m\beta_n\overline{V}_{mn}C_mS_n \\ &+ C_{16}\alpha_m\beta_n\overline{U}_{mn}S_mC_n + C_{16}\alpha_m^2\overline{V}_{mn}S_mC_n\big) \end{aligned} \tag{59}$$

$$\begin{aligned} \sigma_{y,y} = -\sum_{m=1}^{\infty}\sum_{n=1}^{\infty} \big(&C_{12}\alpha_m\beta_n\overline{U}_{mn}S_mS_n + C_{22}\beta_n^2\overline{V}_{mn}S_mS_n \\ &+ C_{26}\beta_n^2\overline{U}_{mn}C_mS_n + C_{26}\alpha_m\beta_n\overline{V}_{mn}C_mS_n\big) \end{aligned} \tag{60}$$

$$\begin{aligned} \tau_{xy,x} = -\sum_{m=1}^{\infty}\sum_{n=1}^{\infty} \big(&C_{16}\alpha_m^2\overline{U}_{mn}C_mS_nC_{26}\alpha_m\beta_n\overline{V}_{mn}C_mS_n \\ &+ C_{66}\alpha_m\beta_n\overline{U}_{mn}S_mS_n + C_{66}\alpha_m^2\overline{V}_{mn}S_mS_n\big) \end{aligned} \tag{61}$$

$$\begin{aligned} \tau_{xy,y} = -\sum_{m=1}^{\infty}\sum_{n=1}^{\infty} \big(&C_{16}\alpha_m\beta_n\overline{U}_{mn}S_mS_n + C_{26}\beta_n^2\overline{V}_{mn}S_mS_n \\ &+ C_{66}\beta_n^2\overline{U}_{mn}C_mS_n + C_{66}\alpha_m\beta_n\overline{V}_{mn}C_mS_n\big) \end{aligned} \tag{62}$$

where, for a harmonic mn,

$$\overline{U}_{mn}(z) = U_{mn} + zX_{mn} + z^3\mathbb{X}_{mn},$$

$$\overline{V}_{mn}(z) = V_{mn} + zY_{mn} + z^3\mathbb{Y}_{mn}$$

and $S_m = \sin\alpha_m x$, $S_n = \sin\beta_n y$, $C_m = \cos\alpha_m x$ and $C_n = \cos\beta_n y$.

References

[1] Crayley EF, De Luis J. Use of piezoelectric actuators as elements of intelligent structures. AIAA J 1987;25:1371–85.
[2] Crawley EF, Anderson EH. Detailed models of piezoceramic actuation of beams. J Intell Mater Syst Struct 1990;1:4–25.
[3] Lee CK. Theory of laminated piezoelectric plates for the design of distributed sensors/actuators. Part 1: Governing equations and reciprocal relationships. J Acoust Soc Am 1990;87:1144–58.
[4] Wang BT, Rogers CA. Laminate plate theory for spatially distributed induced strain actuators. J Compos Mater 1991;25:433–52.
[5] Hwang JH, Wu TL. Analysis of hybrid multilayered piezoelectric plates. Int J Eng Sci 1996;34:171–81.
[6] Ray MC, Rao KM, Samanta B. Exact analysis of coupled electroelastic behavior of piezoelectric plate under cylindrical bending. Comput Struct 1992;45:667–77.
[7] Vel SS, Batra RC. Cylindrical bending of laminated plates with distributed and segmented piezoelectric actuators/sensors. AIAA J 2000;38:857–67.
[8] Vel SS, Batra RC. Exact solution for the cylindrical bending of laminated plates with embedded piezoelectric shear actuators. Smart Mater Struct 2001;10:240–51.
[9] Vel SS, Mewer RC, Batra RC. Analytical solution for the cylindrical bending vibration of piezoelectric composite plates. Int J Solids Struct 2004;41:1625–43.
[10] Mallik N, Ray MC. Exact solutions for the analysis of piezoelectric fiber reinforced composite as distributed actuators for smart composite plates. Int J Mech Mater Des 2005;2:81–97.
[11] Mitchell JA, Reddy JN. A refined hybrid plate theory for composite laminates with piezoelectric laminae. Int J Solids Struct 1995;32:2345–67.
[12] Reddy JN. A simple higher-order theory for laminated composite plates. J Appl Mech 1984;51:745–52.
[13] Liao L, Yu W. An electromechanical Reissner–Mindlin model for laminated piezoelectric plates. Compos Struct 2009;88:394–402.
[14] Dumir PC, Kumari P, Kapuria S. Assessment of third order smeared and zigzag theories for buckling and vibration of flat angle-ply hybrid piezoelectric panels. Compos Struct 2009;90:346–62.
[15] Kumari P, Nath JK, Dumir PC, Kapuria S. An improved third order theory and assessment efficient zigzag theory for angle-ply flat hybrid panels. Compos Struct 2008;83:226–36.
[16] Moita JMS, Soares CMM, Soares CAM. Analyses of magneto-electro-elastic plates using a higher order finite element model. Compos Struct 2009;91:421–6.
[17] Lage RMG, Soares CMM, Soares CAM. Layerwise partial mixed finite element analysis of magneto-electro-elastic plates. Comput Struct 2004;82:1293–301.
[18] Reddy JN. On laminated composite plates with integrated sensors and actuators. Eng Struct 1999;21:568–93.
[19] Torres DAF, Mendonça PTR. Analysis of piezoelectric laminates by generalized finite element method and mixed layerwise-HSDT models. Smart Mater Struct 2010;19:035004.
[20] Reddy JN. Mechanics of laminated composite plates and shells: theory and analysis. Boca Raton: CRC Press; 2004.
[21] Levinson M. An accurate simple theory of the static and dynamics of elastic plates. Mech Res Commun 1980;7:343–50.
[22] Vidoli S, Batra RC. Derivation of plate and rod equations for a piezoelectric body from a mixed three-dimensional variational principle. J Elast 2000;59:23–50.
[23] Saravanos DA, Heyliger PR, Hopkins DA. Layerwise mechanics and finite element for the dynamic analysis of piezoelectric composite plates. Int J Solids Struct 1997;34:359–78.
[24] Lee HJ. Finite element analysis of active and sensory thermopiezoelectric composite materials. Glenn Research Center – National Aeronautics and Space Administration – Report 210892; 2001.
[25] Machado MAM. Analytical solutions for rectangular piezoelectric laminated plates. MSc dissertation, Technology Institute of Aeronautics – ITA; 2004 (in Portuguese).
[26] Correia VMF, Gomes MAA, Suleman A, Soares CMM, Soares CAM. Modelling and design of adaptive composite structures. Comput Methods Appl Mech Eng 2000;185:325–46.